

**USE OF MICROEMULSIONS CONTAINING SHORT CHAIN  
ANIONIC AND CATIONIC SURFACTANT FOR ENHANCED OIL  
RECOVERY (EOR)**

By

**Fuad Shamel Habjouqa**

Supervisor

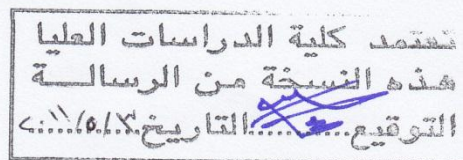
**Dr. Abeer Al-Bawab, Prof.**

Co-Supervisor

**Dr. Ibrahim Kayali, Prof.**

**This Thesis was Submitted in Partial Fulfillment of the Requirements  
for the Master's Degree of Science in Chemistry**

**Faculty of Graduate Studies  
The University of Jordan**



**May, 2011**



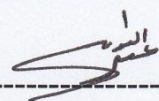
## COMMITTEE DECISION

**This Thesis (Use of Microemulsions Containing Short Chain Anionic and Cationic Surfactant for Enhanced Oil Recovery (EOR)) was Successfully Defended and Approved on 20/4/2011**

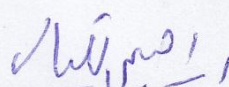
### Examination Committee

### Signature

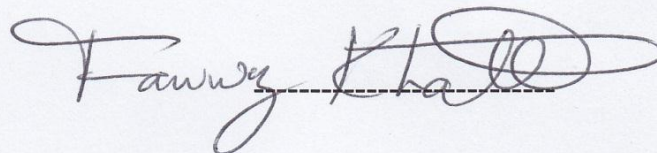
Dr. Abeer Al-Bawab, (Supervisor)  
Prof. of Physical Chemistry



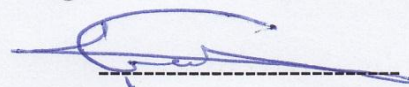
Dr. Ibrahim Kayali, (Co-Supervisor)  
Prof. of Physical Chemistry  
(Al-Quds University)



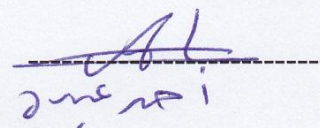
Dr. Fawwaz Khalili, (Member)  
Prof. of Inorganic and nuclearchemistry




Dr. Fadwa Odeh, (Member)  
Assistant Prof. of Physical Chemistry



Dr. Ahmad Abdo, (Member)  
Ph.D. of Physical Chemistry  
(Vivid Separation and Filtration Company)



تمت كلية الدراسات العليا  
هذه النسخة من الرسالة  
التوقيع:  التاريخ: 20/4/2011

DEDICATION

*For my Dad and Mom...*

*For my Sister...*

*Thank you for your prayers, love and support*

## ACKNOWLEDGEMENT

First, I would like to thank my advisor Prof. Abeer Al-Bawab and my co-advisor Prof. Ibrahim Kayali for their great support and extreme patience with me.

I also would like to express my appreciation for Prof. Fawwaz Khalili for his support and help throughout my master's study.

I gratefully acknowledge Miss Ayat Bozeya and Dr. Juma'a Kafawein for their extreme help and nothing of this work might have been done without their support, and also for being very supportive any time I seek their help.

I also would like to acknowledge Jordan Petroleum Refinery Company for supporting me with the crude oil, Hamdi Mango Center for Scientific Research for providing a very suitable and well-equipped working environment, where all the experiment took place in their laboratory, and the Deanship of Academic Research of the University of Jordan for funding this research.

I would like to thank all my friends for their prayers and being not only the best friends, but also the best brothers and sisters a man can ever have in his lifetime.

A very special appreciation goes to my parents; my mother, my father and my sister; without their limitless support and love, I would not be able to move forward.

My ultimate appreciation is for Allah, he always gives me strength to overcome any obstacle, and he answers my prayers and always chose the best for me.

## Contents

<i>DEDICATION</i> .....	iii
ACKNOWLEDGEMENT .....	iv
LIST OF TABLES .....	vii
LIST OF FIGURES .....	viii
LIST OF ABBREVIATIONS .....	x
ABSTRACT .....	xi
1. INTRODUCTION .....	1
1.1. Crude Oil and Oil Recovery.....	1
1.1.1. EOR .....	1
1.2. Surfactants.....	2
1.2.1. Classification of surfactants.....	4
1.2.2. Properties of surfactant .....	5
1.2.2.1. Surface adsorption .....	5
1.2.2.2. Self-assembly.....	6
1.3. Emulsions and Microemulsions. ....	10
1.3.1. Emulsion (Em).....	10
1.3.2. Microemulsion (ME) .....	10
1.4. Phase Diagram .....	11
1.4.1. Phase diagram determination.....	12
1.4.2. Winsor phases .....	14
1.5. ME and EOR .....	16
1.5.1. ME and IFT.....	16
1.5.2. ME and surfactants .....	16
1.6. Extended surfactant.....	17
2. LITERATURE REVIEW.....	23
2.1.1. Carbon dioxide (CO <sub>2</sub> ) Injection .....	23
2.1.2. Alkaline solutions .....	23
2.1.3. Polymers in EOR .....	24
2.2. Surfactant in EOR .....	24
2.2.1. Temperature effect.....	25
2.2.2. Chain effect (Extended Surfactants).....	25
2.2.3. Salinity effect.....	27
2.2.4. Co-surfactant effect .....	29

2.2.4.1. Alcohol using.....	29
3. MATERIALS AND METHODS.....	32
3.1. Materials.....	32
3.2. Instrumentation .....	32
3.3. Methods.....	33
3.3.1. Preparing the Surfactant .....	33
3.3.2 Phase Diagram Determination.....	33
3.3.3. Salinity Scan .....	35
3.3.4. IFT measurements .....	35
4. Results and Discussion.....	37
5. Conclusion .....	50
Future Work .....	51
References .....	52
Abstract in Arabic.....	56

## LIST OF TABLES

<b>Table No</b>	<b>Table Title</b>	<b>page</b>
Table 1	Properties of Em and ME (Huang, 1995)	11
Table 2	Mass and percent for $(L_{123} - 4S)^{\otimes}$ and water used in phase diagram determination	34
Table 3	Mass and percent for 65% $(L_{123} - 4S)^{\otimes}$ and n-decane used in phase diagram determination	35
Table 4	Phase behavior of $(L_{123} - 4S)^{\otimes}$ with 1:1M TBAB in various NaCl %	44

## LIST OF FIGURES

Figure No.	Figure Title	Page
Figure 1	Surfactant molecule	3
Figure 2	Classification of surfactants (Pashley and Karaman, 2004)	5
Figure 3	Schematic diagram of surfactant molecules adsorbed at water/air interface	6
Figure 4	Schematic diagram of surfactant micelle (Pashley and Karaman, 2004)	8
Figure 5	Use of the critical packing parameter to predict aggregate structures (Pashley and Karaman, 2004)	9
Figure 6	Gibb's triangle diagram	11
Figure 7	Schematic diagram of the types of structures formed at different compositions of oil, water and surfactant	13
Figure 8	Phase diagrams transformed from Winsor I (a,b) via Winsor III (c, d, e) to Winsor II (f, g). The dark triangle is the three phase region	14
Figure 9	Phase changes from Winsor I $\rightarrow$ III $\rightarrow$ II of a system containing low amount of surfactant and equal amount of oil and water	15
Figure 10	Schematic shows the surface tension of a liquid (Raymond et al. 2006)	18
Figure 11	(a) Two droplets in the spinning drop chamber. (b) After deformation to the quasi-static situation ( $R_c$ contact radius, $R_d$ outer radius). (c) After coalescence (Schoolenberg and During 1997)	20
Figure 12	Spinning Drop Technique Apparatus (Schoolenberg and During 1997)	22
Figure 13	Structure of extended surfactant X-AES (Klaus <i>et al.</i> , 2009)	27
Figure 14	Effect of NaCl (0.5%) on phase behavior (Nedjhioui <i>et al.</i> 2007)	28
Figure 15	Fish diagram of the $C_{12,13}-(PO)_8-SO_4Na$ , brine/hexadecane ME at constant $27^\circ C$ and equal volume of oil to water (Sabatini <i>et al.</i> , 2009)	28
Figure 16	effect of adding cationic surfactant on IFT (Kayali <i>et al.</i> 2010)	30
Figure 17	The partial ternary phase diagram of the system $(L_{123}-4S)^{\otimes}$ , water and decane	38
Figure 18	Lamellar liquid crystal, $L_\alpha$	39
Figure 19	The phase diagram of the system $(L_{123}-4S)^{\otimes}$ : TBA, water and decane	40
Figure 20	The three phase region in $(L_{123}-4S)^{\otimes}$ : TBA, water and decane system, showing the bluish middle phase	41
Figure 21	The three phase region in $(L_{123}-4S)^{\otimes}$ , water and decane system	41
Figure 22	Salinity scan containing 0.5 wt % $(L_{123}-4S)^{\otimes}$ , TBAB (1:1 M ratio) with (WOR=1).	42
Figure 23	Salinity scan containing 1.0 wt % $(L_{123}-4S)^{\otimes}$ , TBAB (1:1 molar ratio) with (WOR=1) and decane	43



Figure 24	Salinity scan containing 0.5 wt% (L <sub>123</sub> -4S) <sup>®</sup> with (WOR=1) in absence of TBAB	44
Figure 25	IFT for the system 1.0 wt% (L <sub>123</sub> -4S) <sup>®</sup> , TBAB (1:1), decane	45
Figure 26	The salinity scan behavior after a period of time, showing two phase oil and liquid	48
Figure 27	Salinity scan containing 1.0 wt% (L <sub>123</sub> -4S) <sup>®</sup> , TBAB (1:1 molar ratio) with (WOR =1) and crude oil	49

### LIST OF ABBREVIATIONS

<b>CMC</b>	Critical micelle concentration
<b>Em</b>	Emulsion
<b>EOR</b>	Enhanced oil recovery
<b>IFT</b>	Interfacial tension
<b>ME</b>	Microemulsion
<b>O/W</b>	Oil in water
<b>PO</b>	Polypropylene oxide
<b>SDT</b>	Spinning drop technique
<b>SEAR</b>	Surfactant enhanced aquifer remediation
<b>SF</b>	Surface tension
<b>TBAB</b>	Tetrabutyl ammonium bromide
<b>WOR</b>	Water/Oil weight ratio

# Use of Microemulsions Containing Short Chain Anionic and Cationic Surfactant for Enhanced Oil Recovery (EOR)

By

**Fuad Shamel Habjouqa**

Supervisor

**Dr. Abeer Al-Bawab, Prof.**

Co-Supervisor

**Dr. Ibrahim Kayali, Prof.**

## ABSTRACT

The partial ternary phase diagrams of anionic extended surfactant of alkyl polypropylene oxide (PO) sulfate  $C_{12}(PO)_4SO_4$  alone was studied while the second phase diagram was combined with the cationic hydrotrope, tetrabutyl ammonium bromide (TBAB) in presence of water and n-decane, They were determined under ambient conditions. Middle phase microemulsion was formulated using salinity scans in the dilute regions of surfactant/brine/n-decane. Visual inspection as well as cross polarizer and optical microscopy were used to detect anisotropy. Spinning drop technique was used to measure interfacial tension (IFT). The first ternary phase diagram using the extended surfactant alone showed two one phase regions, the anisotropic lamellar liquid crystalline phase,  $L_\alpha$  and the sponge phase  $L_3$ . In addition to three phase region which consist of an emulsion between two transparent liquids. In the second ternary phase diagram using the extended surfactant combined with TBAB a new isotropic micellar region,  $L_1$ , appeared. Meanwhile the  $L_\alpha$  and  $L_3$  phases disappeared completely and the three phase region had a bluish transparent middle phase. IFT measurements between middle phase and brine and between n-decane and brine yielded ultralow values. The value of IFT suggested high rigidity due to the steric hindrance caused by the presence of PO groups inside the extended surfactant. Calculated IFT values using the characteristic length obtained using De Gennes approximation gave almost half the measured values. The salinity scan of the crude oil shows that this method can be used in Enhanced oil recovery (EOR).

## 1. INTRODUCTION

### 1.1. Crude Oil and Oil Recovery

Crude oil is a flammable liquid that is found in geologic formations beneath the Earth's surface, which consists of a mixture of hydrocarbon molecules and lesser quantities of organic molecules containing sulfur, nitrogen, oxygen, and some metals. Its density is commonly less than water. The oil is an important essential source of energy in our life. Oil is recovered mostly through oil drilling in a process called oil recovery. This process can be divided into three categories: primary, secondary, and **Enhanced Oil Recovery (EOR)**. In the primary process oil is forced out from the reservoir by the natural pressure of the trapped fluid inside the reservoir. When the pressure is reduced to a point where it is no more effective, water is injected to increase the pressure in a secondary recovery process. The first and second process can extract 15-40% of oil from the well. EOR is used as a third process (Donaldson *et al.*, 1989) (Gluyas and Swarbrick, 2004).

#### 1.1.1. EOR

EOR is a generic term for techniques used for increasing the amount of crude oil that extracted from an oil field. By using EOR 35-60% of the original oil can be extracted. EOR is divided into four methods:

**a) Thermal method:** in this method, crude oil is heated by many methods to reduce its viscosity and/or vaporize part of the oil, such as steam injection, which had been used commercially since the 1960's (Donaldson *et al.*, 1989).

**b) Gas injection:** carbon dioxide, natural gas or nitrogen, is injected inside the reservoir to reduce the viscosity of the crude oil when the gas is mixed with it. Air cannot be used here because the oil may be ignited (Donaldson *et al.*, 1989).

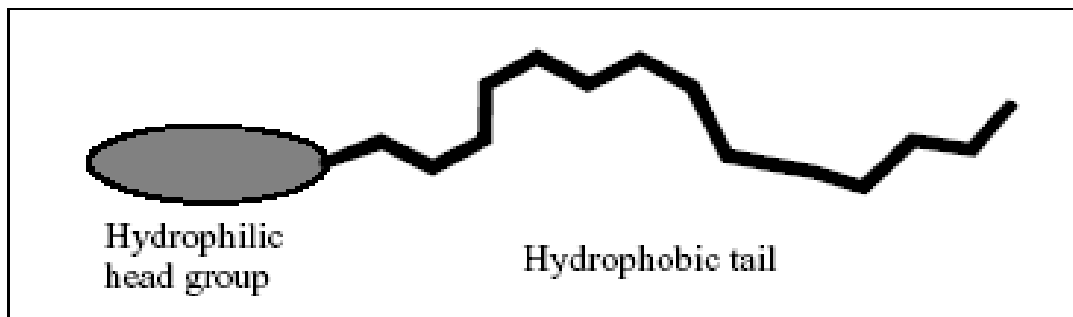
**c) Microbial injection:** it is a recent method which uses strains of microbes that have been discovered and developed (using gene mutation), which function either by partially digesting long hydrocarbon molecules, or by generating biosurfactants, or by emitting carbon dioxide (which then functions as gas injection method) (Kang *et al.*, 2001) (Rafael and Radolfo, 2004).

**d) Chemical injection:** several chemicals, usually diluted solutions, are used for EOR. Alkaline solutions are used to convert the organic acids in oil to soap that may lower the interfacial tension (IFT) enough to increase the production. Dilute solution of soluble polymer can increase the viscosity of injected water, which increases the oil recovered. **Surfactants** are used to lower the IFT that impedes oil droplets from moving through a reservoir by formulating **Microemulsions** (ME) (Donaldson *et al.*, 1989).

## 1.2. Surfactants

The name 'surfactant' refers to molecules that are 'surface-active'. Surfactants are usually organic compounds that are amphiphilic, meaning that they contain both hydrophobic groups "Tail" which is hydrocarbon soluble (non-polar), and hydrophilic groups "Head" which is water soluble (polar). Therefore, they are soluble in organic solvents and water (Figure 1).





**Figure 1:** Surfactant molecule

Because of its dual affinity, surfactant molecule does not feel "at ease" in any solvent, since there is always one of the groups which "does not like" the solvent environment. This is why surfactants molecules exhibit a very strong tendency to migrate to interfaces or surfaces or to self-organize in oil and water systems, and to orient so that the hydrophilic groups lie in water and the hydrophobic groups are placed out of it. Due to the migration of the surfactant molecule to the surface or interfaces, they reduce the surface tension of water by adsorbing at the liquid-air interface (surface of water), and also reduce the interfacial tension between oil and water by adsorbing at the liquid-liquid interface (Holmberg *et al.*, 2002) (Salager, 1999).

Surfactant compounds play an important role in many practical applications and products. They are often labeled according to their main use such as: soap, detergent, wetting agent, dispersant, emulsifier, foaming agent, bactericide, corrosion inhibitor and antistatic agent (Rieger *et al.*, 1997).

### 1.2.1. Classification of surfactants

Surfactants (Figure 2) are classified to:

- 1) **Anionic surfactants**, which dissociate in water to amphiphilic anion, and a cation, generally  $\text{Na}^+$ ,  $\text{K}^+$ , or  $\text{NH}_4^+$ . They are the most commonly used in our life, such as soap (sodium salty fatty acid), foaming agent (sodium lauryl sulfate), detergent (sodium alkyl benzene sulfonates), and wetting agent (dialkylsulfosuccinates). (Bozey 2008) (Pashley and Karaman, 2004).
- 2) **Cationic surfactants**, which dissociate in water to amphiphilic cation, and anion basically halogen. Most of cationic surfactants are based on nitrogen compounds such as amines, and quaternary ammonium compounds. But amines are only used as a surfactant in the protonated state, so they cannot be used at high pH. On the other hand quaternary ammoniums are not pH sensitive. Common cationic surfactants are more expensive than the anionic ones, because of the high-pressure of hydrogenation reaction that must be carried out during their synthesis (Pashley and Karaman, 2004) (Bozey 2008).
- 3) **Zwitterionic surfactants (amphoteric)** have cationic and anionic amphiphile upon dissociation. Ammonium is almost the main source of the positive charge, and carboxylate is by far the most common source for the negative charge although the sources may vary. Due to amphoteric property of the surfactant, it changes from net anionic via zwitterionic to cationic on going from high to low pH. Neither the base nor the acid site is permanently charged, i.e. the compound is only zwitterionic over a certain pH range. Phospholipids and N-alkyl derivatives of simple amino acid (e.g. glycine) are common types of zwitterionic surfactants (Pashley and Karaman, 2004).

4) **Nonionic surfactants**, where the hydrophilic part has a non-dissociable groups such as alcohol, phenol, ester, ether, and amide (Pashley and Karaman, 2004).

---

<b>ANIONIC:</b>	
Sodium dodecyl sulphate (SDS)	$\text{CH}_3(\text{CH}_2)_{11}\text{SO}_4^-\text{Na}^+$
Sodium dodecyl benzene sulphonate	$\text{CH}_3(\text{CH}_2)_{11}\text{C}_6\text{H}_4\text{SO}_3^-\text{Na}^+$
<b>CATIONIC:</b>	
Cetyltrimethylammonium bromide (CTAB)	$\text{CH}_3(\text{CH}_2)_{15}\text{N}(\text{CH}_3)_3^+\text{Br}^-$
Dodecylamine hydrochloride	$\text{CH}_3(\text{CH}_2)_{11}\text{NH}_3^+\text{Cl}^-$
<b>NON-IONIC:</b>	
Polyethylene oxides	e.g. $\text{CH}_3(\text{CH}_2)_7(\text{O}.\text{CH}_2\text{CH}_2)_8\text{OH}$ (called $\text{C}_8\text{EO}_8$ )
<b>ZWITTERIONIC:</b>	
Dodecyl betaine	$\text{C}_{12}\text{H}_{25}\text{N}^+ \begin{cases} (\text{CH}_3)_2 \\ \text{CH}_2\text{COO}^- \end{cases}$
Lecithins, e.g. phosphatidyl choline	$  \begin{array}{c}  \text{O} \\  \parallel \\  \text{CH}_2\text{OCR} \\    \\  \text{O} \\  \parallel \\  \text{CHOOCR} \\    \\  \text{O} \\  \parallel \\  \text{CH}_2\text{OP-O-CH}_2\text{-N}^+(\text{CH}_3)_3 \\    \\  \text{O}^-  \end{array}  $

---

**Figure 2.** Classification of surfactants (Pashley and Karaman, 2004)

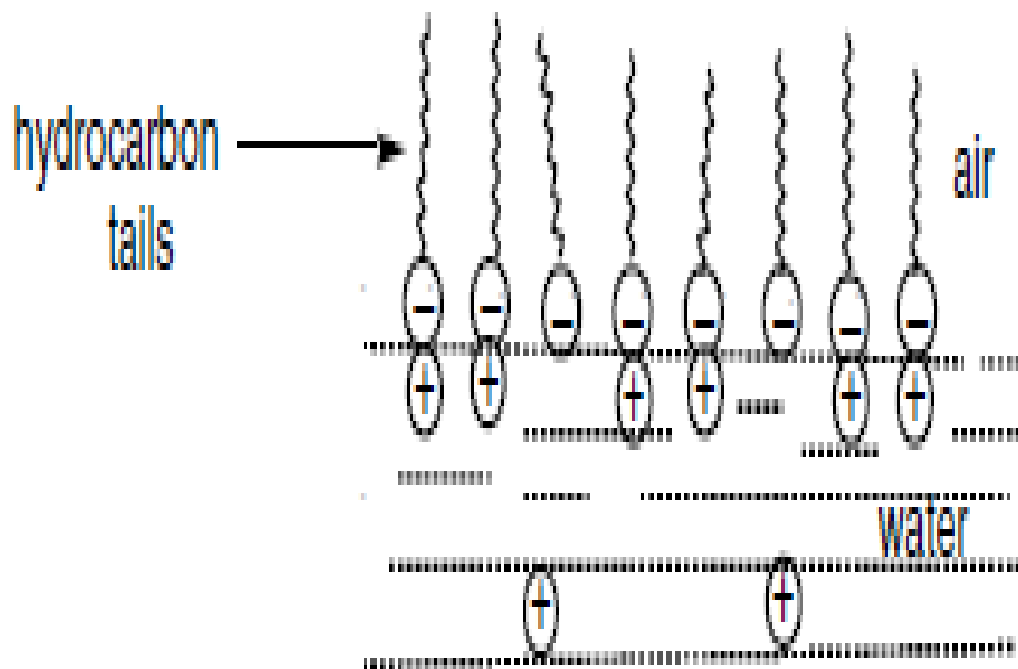
### 1.2.2. Properties of surfactant

Because of the structure of the surfactants, their solutions have two common properties: surface adsorption, and the ability to self assemble.

#### 1.2.2.1. Surface adsorption

When dissolving a surfactant, the hydrophilic part dissolves in water, while the hydrophobic part (hydrocarbon chain) is insoluble, therefore the surfactant molecules can adsorb and orientate at air/solution interface such as in Figure 3. By this orientation, the

surface tension of water is reduced and the surface now appear more hydrophobic. (Pashley and Karaman, 2004).



**Figure 3.** Schematic diagram of surfactant molecules adsorbed at the water/air interface.

#### 1.2.2.2. Self-assembly

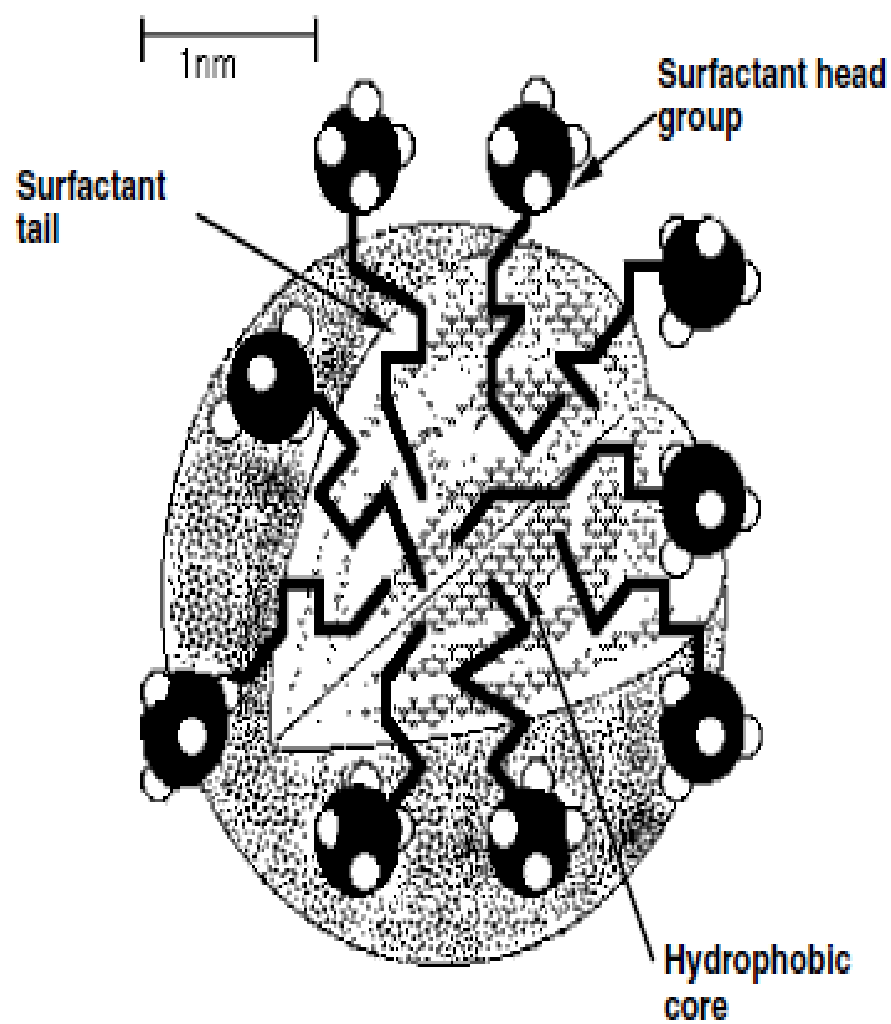
By increasing the surfactant's concentration, and because of surfactants' dual character property, its molecules have a remarkable ability to self-assemble (aggregate) in solutions, forming a wide variety of equilibrium phase structures, in which likes is associated with likes, when dispersed in water or in water oil systems, *e.g.* micelles.

**Micelles** are the simplest example to understand these formations. The hydrocarbon chain of surfactants is insoluble in water which causes the molecules to concentrate at the air/water interface. Adding surfactant would decrease the surface tension of water. As the surfactant concentration increases, the surface reaches saturation and surface tension

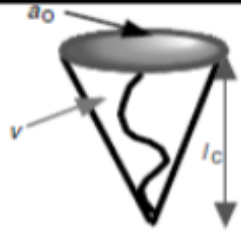
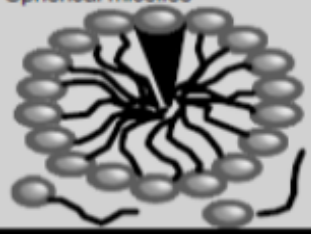

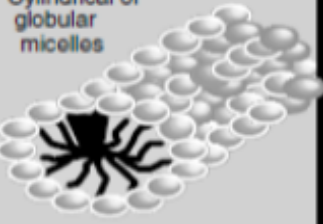

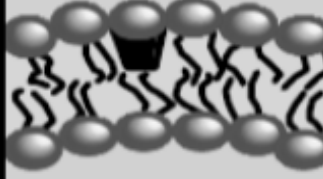

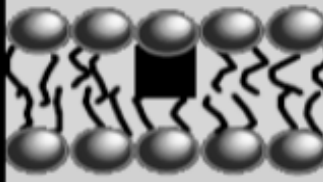

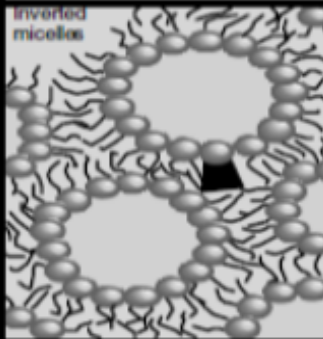
remain virtually unchanged. At this point it reaches critical micelle concentration (CMC), which is the point when the surfactant molecules undergo self-assembly to create a phase in which the hydrophobic tails orient themselves inside the aggregate and the polar head groups orient themselves toward the aqueous phase (Figure 4) (Pashley and Karaman, 2004).

To understand the change in the aggregate structure, the critical packing parameter can be used which is  $v/(a^*l)$ , where  $v$  is the volume of the surfactant tail,  $a$  is the surfactant area per molecule, and  $l$  is the length of the surfactant hydrophobic part. Critical packing value suggests the structure of the aggregate, e.g. value less than 1/3 suggests a spherical micelle. Aggregate structure is influenced by the addition of an electrolyte, addition of co-surfactant, change in temperature, change in counterion, or insertion of unsaturated or branched chains. Some of the basic structures are shown in Figure 5. e.g. value of the critical packing parameter more than 1 suggests inverted micelle.





**Figure 4.** Schematic diagram of a surfactant micelle (Pashley and Karaman, 2004)

Lipid	Critical packing parameter	Critical packing shape	Structures formed
Single-chained lipids with large head-group areas. e.g. NaDS in low salt	$< 1/3$		Spherical micelles 
Single-chained lipids with small head-group areas e.g. NaDS in high salt	$1/3 - 1/2$		Cylindrical or globular micelles 
Double-chained lipids with large head-group and fluid chains e.g. lecithin	$1/2 - 1$		Flexible bilayers, vesicles 
Double-chained lipids with small head-group areas: anionic lipids high salt. e.g. phosphatidyl ethanolamine	$\sim 1$		Planar bilayers 
Double-chained lipids having small head groups e.g. non-ionic lipids	$> 1$		Inverted micelles 

**Figure 5.** Use of the critical packing parameter to predict aggregate structures (Pashley and Karaman, 2004)

### 1.3. Emulsions and Microemulsions.

Water, surfactant, and hydrocarbon oil can form structures called emulsion and microemulsion.

#### 1.3.1. Emulsion (Em)

Em is a mixture of two or more immiscible liquids, which is a suspension of small globules of one liquid (disperse) in a second liquid (continuous) to form droplets. *e.g.* oil in vinegar. However, these droplets are unstable, because of the high interfacial energy, and they will destabilize quickly and separate into oil and vinegar phases. The stability of an emulsion can be enhanced by adding surfactants (emulsifier) to the system which reduce the interfacial energy of the droplets. Simple emulsions are classified into two types: oil-in-water (O/W) normal Em (oil dispersed in water) or water-in-oil (W/O) reversed Em (water dispersed in oil) (Holmberg *et al.*, 2002).

#### 1.3.2. Microemulsion (ME)

ME are formed when surfactants reduce the oil/water interfacial tension to ultra low values, allowing thermal motions to be dispersed spontaneously into the two immiscible phases, and solutions are all isotropic and transparent in appearance. In many cases, a second surfactant, also called co-surfactant, such as a medium chained alcohol, is required. In the case of other surfactants, addition of salt can form ME (Holmberg *et al.*, 2002).

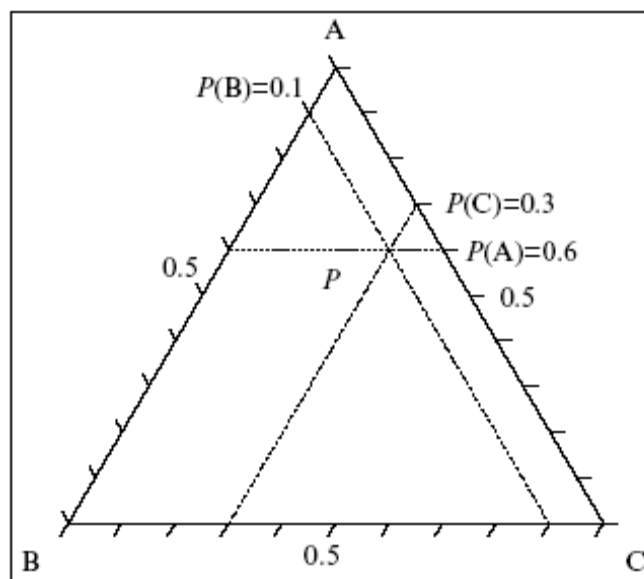
ME and Em are fundamentally different (Table 1), and ME should not be regarded as Em with small droplets. Em are unstable and will eventually separate into phases, while ME are thermodynamically stable with a very high degree of dynamics with regards to the internal structure. (Huang 1995) (Holmberg *et al.*, 2002).

**Table 1.** Properties of Em and ME (Huang 1995)

Property	Em	ME
Appearance	Turbid	Transparent
Droplet size	0.1-100 $\mu\text{m}$	1-100 nm
Formation	Stirring, etc.	Spontaneous
Thermodynamic Stability	Unstable	Stable

### 1.4. Phase Diagram

A triangular three-phase diagram is used to determine the structures that may be formed from different composition of oil, water and surfactant. Each edge of the triangle represents one of the pure compounds, namely 100%. Any point at the axes between two edges represents the % of two compounds and 0 % of the third compound. Any point inside the phase diagram represents a three component sample with total percent of 100 % (Figure 6).

**Figure 6.** Gibb's triangle diagram

There is a fundamental rule to understand the phase diagram (Gibb's phase rule):

$$F = C - P + 2$$

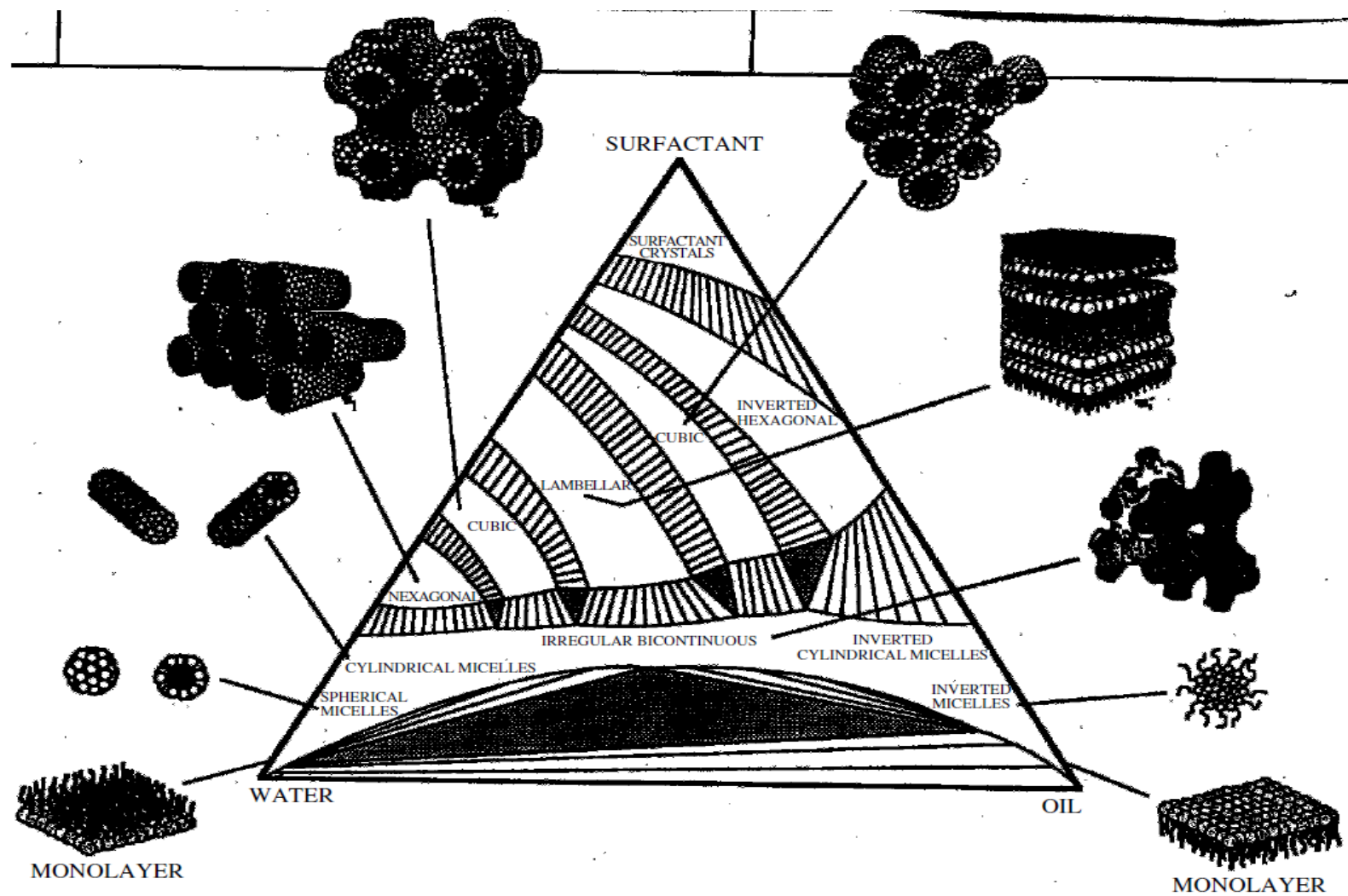
Where (F) is the degree of freedom, which consists of pressure, temperature, and composition, (C) is the number of components are used in the system, (P) is the number of phases that exists in the system. For example, when temperature and pressure are kept constant, a three component system in a three phase region will have no degree of freedom, that is, no composition change for any component (Huang 1995).

#### 1.4.1. Phase diagram determination

To determine a phase diagram of three-component system, a large numbers of two component samples with different compositions (usually by mass %) must be prepared. Considering whether there is a single homogenous phase or more than one phase, then allow the sample to be separated which often is possible by centrifugation. Then a third compound will be added gradually to the samples, and then observing the changes that might occur upon each addition. Finally, determine the phases, there regions and compositions (Holmberg *et al.*, 2002).

In the oil / surfactant / water systems, due to the surfactant aggregates, different types of phases can be found in such systems (Figure 5), one phase (ME, liquid crystal phase), two phase (Em, or solid and liquid), three phase (three liquids, liquid crystal with two liquids, solid with two liquids, solid with liquid with liquid crystal) regions. ME region can be determined by visual observation of clearness/turbidity change, the liquid crystalline phase can be identified by its optical pattern in between a crossed polarizers. Further identification can be achieved by X-ray (Huang 1995) (Laidler *et al.*, 2003).

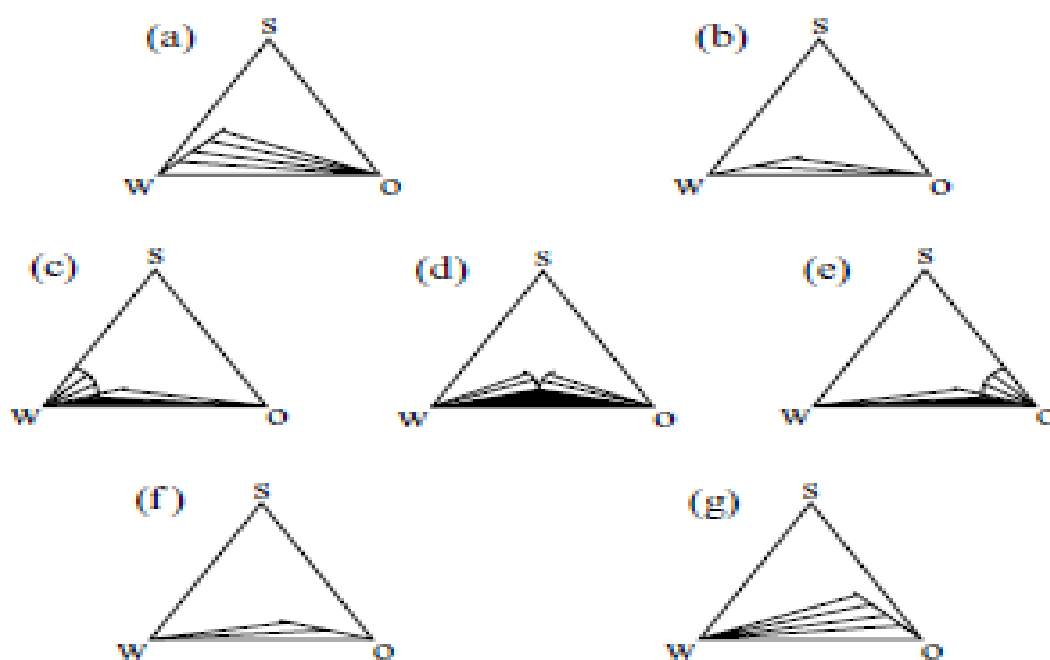




**Figure 7.** Schematic diagram of the types of structures formed at different compositions of oil, water and surfactant.

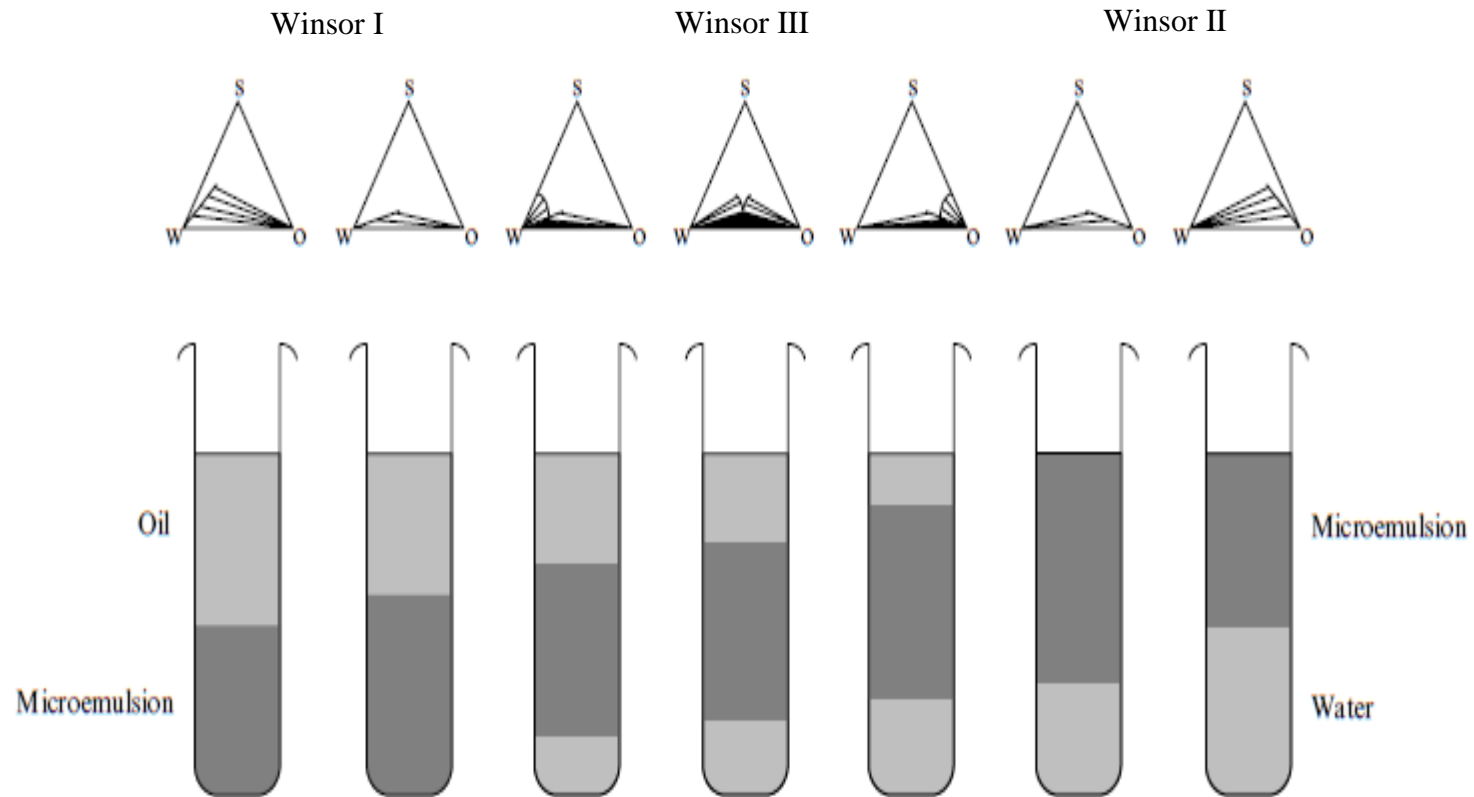
### 1.4.2. Winsor phases

At low surfactant concentrations, there is a sequence of equilibria between phases, commonly known as Winsor phases. **Winsor I** (lower phase ME), which is a ME phase that maybe in equilibrium with excess oil. **Winsor II** (upper phase ME), a ME in equilibrium with excess water, and **Winsor III** (middle phase ME), a ME equilibrium with both excess phases (water and oil) (Figure 8) (Holmberg *et al.*, 2002).



**Figure 8.** Phase diagrams transformed from Winsor I (a,b) via Winsor III (c,d,e) to Winsor II (f,g). The dark triangle is the three phase region. (Holmberg *et al.*, 2002).

The transition from **I**  $\rightarrow$  **III**  $\rightarrow$  **II** for non-ionic surfactant may occur by raising the temperature, while the transition for ionic surfactant systems containing an electrolyte may be induced by increasing salinity as shown in Figure 9.



**Figure 9.** Phase changes from Winsor **I** → **III** → **II** of a system containing low amount of surfactant and equal amount of oil and water. (Holmberg *et al.*, 2002).

## 1.5. ME and EOR

Oil fields are consisting of porous rocks, usually sandstone and limestone, the pores are filled with brine and petroleum, the permeability depends on the pore size, which is around 50-1000 nm. In oil field, 55-80% of the well is occupied by oil, 10-25% by brine, and the rest is vacant. After the first and second recovery process, high viscous and the oil trapped in porous rocks, and to increase the production of oil we need to reduce the oil/water IFT to ultra low values of the order of  $10^{-3}$  mN/m. ME were interesting in EOR because of their ability to do that (Holmberg *et al.*, 2002).

### 1.5.1. ME and IFT

The IFT values were found to decrease as moves from Winsor I  $\rightarrow$  III, and at minimum at the middle of Winson III region, and increase as it moves to Winson II region. As described before we can move through Winsor I  $\rightarrow$  III  $\rightarrow$  II by increasing the temperature using non-ionic surfactants system, and by increasing the salinity using an ionic surfactants system (Holmberg *et al.*, 2002).

### 1.5.2. ME and surfactants

In order to make ME with low IFT values, surfactants must display the following properties:

- a) Do not precipitate in hard water.
- b) Do not adsorb extensively at the mineral surface of the reservoir.
- c) Form Winsor III with the specific reservoir oil, brine, and temperature.
- d) Stable for an extended period inside reservoir conditions (Holmberg *et al.*, 2002).

In order to increase the efficiency of ME many things had been done, such as (a) Adding water-soluble polymer with similar charge to the surfactant in order to decrease the CMC. (b) Using alcohol as a co-surfactant or as a co-solvent. Nowadays it is not favorable to use alcohol because of its volatility, flammability and toxicity and recently some experiments shown that IFT increased, and solubilization reduced when using alcohols. c) Using a short chain cationic surfactant. d) Extending the surfactant *e.g.* branching the chain of ether sulfonate (Hirasaki *et al.*, 2002) (Ibrahim *et al.*, 2010) (Holmberg *et al.*, 2002).

### **1.6. Extended surfactant**

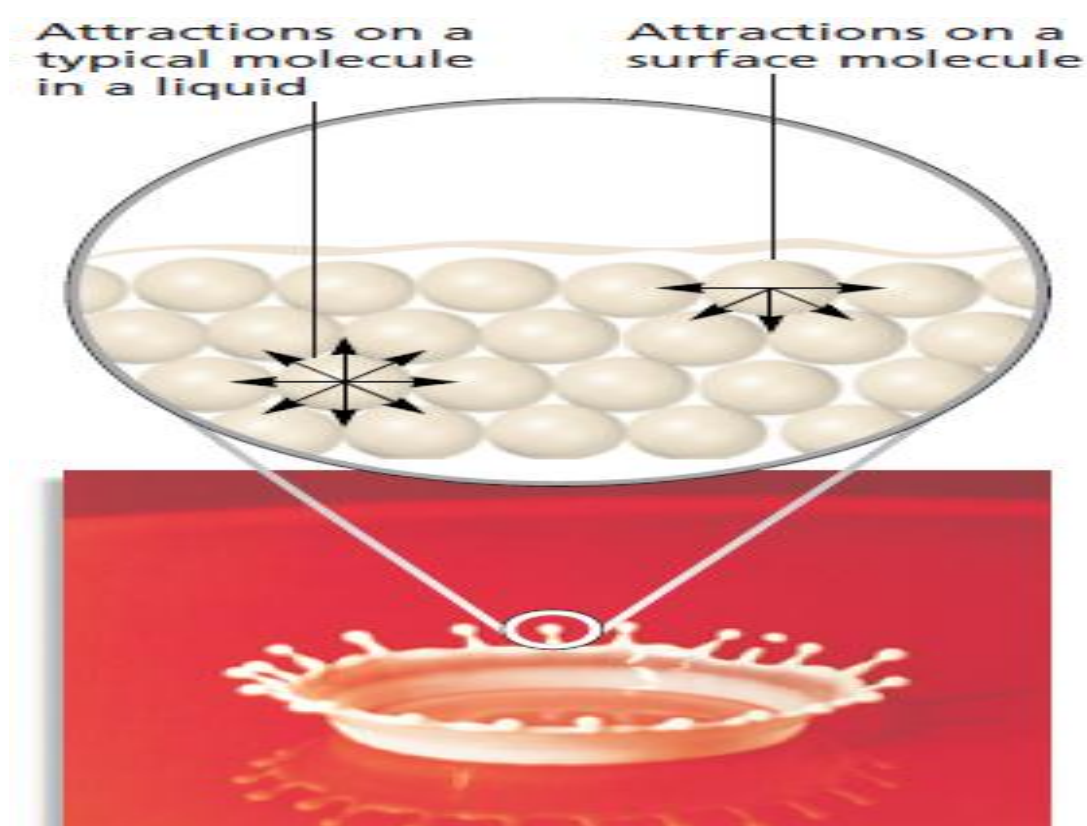
Several investigators reported the ability of the “extended surfactant” to significantly lower CMC compared to values obtained for conventional surfactants (Witthayapanyanon *et al.*, 2010).

Recently, particular attention has been given to a new class of surfactant that has a polypropylene oxides or copolymers of propylene oxides and ethylene oxides inserted between the polar head and the non-polar tail of the conventional surfactant. Such molecular structure with a region of intermediate polarity should enable the surfactant to stretch out further into both water and oil phases thus providing a smooth transition across the interface that would result in reducing IFT even at very low surfactant concentration. These are attractive properties and desirable in many practical applications ranging from pharmaceutical and cosmetic products to EOR and surfactant enhanced aquifer remediation (SEAR).



## 1.7. Surface Tension (SF) and IFT

SF is a force that tends to pull adjacent parts of liquid's surface together, thereby decreasing surface area to the smallest possible size. Surface tension results from the attractive forces between particles of a liquid. The higher the force of attraction, the higher the surface tension. IFT is somewhat similar to SF, while cohesive forces are also involved. However the main forces involved in IFT are adhesive forces (tension) between the liquid phase of one substance and either a solid, liquid or gas phase of another substance. For example, water has a higher surface tension than most liquids. This is due in large part to the hydrogen bonds water molecules can form with each other. (Raymond *et al.* 2006)



**Figure 10.** Schematic shows the surface tension of a liquid. (Raymond *et al.* 2006)

### 1.7.1. Measuring SF and IFT

The surface tension manifests itself in various effects so it offers a number of paths to be measured. Each method depends upon; the nature of the liquid is measured, the stability of its surface when it is deformed, and the conditions under which its tension is to be measured. There are many methods to measure SF such as:

1) Du Noüy Ring method: the traditional method used to measure surface or interfacial tension. Wetting properties of the surface or interface have little influence on this measuring technique. Maximum pull exerted on the ring by the surface is measured (Erbil 2006).

2) Wilhelmy plate method: a universal method used to check surface tension over long time intervals. A vertical plate of known perimeter is attached to a balance, and the force due to wetting is measured (Erbil 2006).

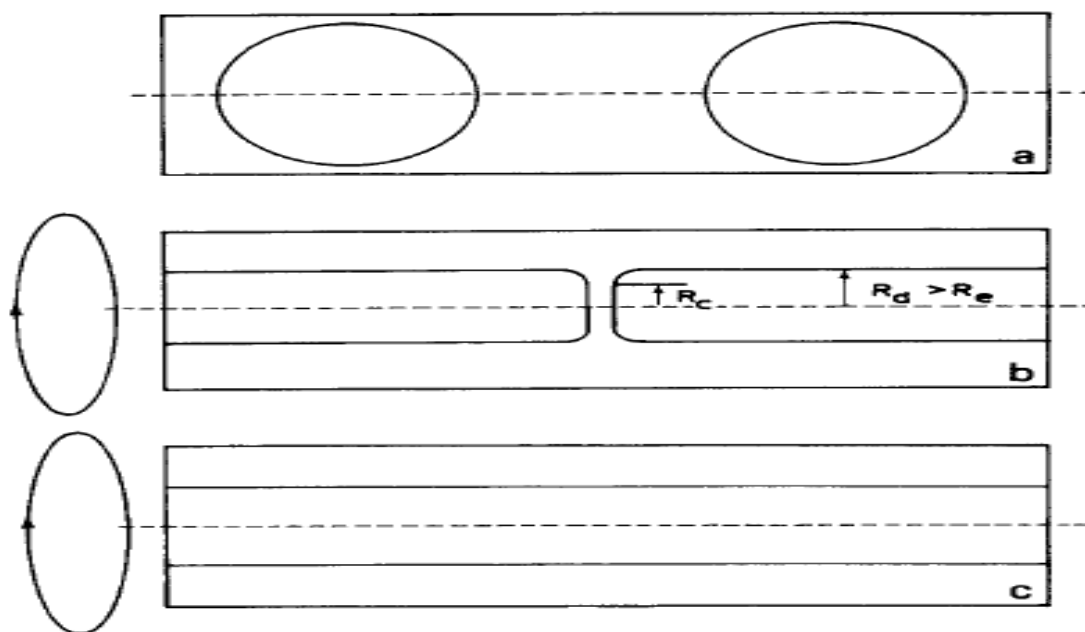
3) Bubble pressure method (Jaeger's method): a measurement technique for determining surface tension at short surface ages. Maximum pressure of each bubble is measured (Erbil 2006)

4) Spinning drop Technique (SDT) method: this technique is ideal for measuring low interfacial tensions. The diameter of a drop within a heavy phase is measured while both are rotated (Schoolenberg and During 1997)

In this investigation the SDT method will be used for IFT measurements.

### 1.7.2. SDT method

In SDT, a droplet of one liquid is surrounded by a second. The liquids are contained in a transparent cylinder which is rotated at a fixed speed. Centrifugal force field will be produced which drives denser liquid to the cylinder perimeter and the less dense liquid to its axis. A cylinder of the lower density material with a concentric shell of the higher density material would arise, were it not for the counteracting effect of the interfacial tension of the two liquids. This minimizes the interfacial energy and drives the droplet in the direction of the spherical shapes it would obtain under quiescent conditions. After some time the droplet reaches an equilibrium shape (Figure 11) under the action of the two opposing driving forces. For large droplets, this shape approximated by a long cylinder with rounded ends (Schoolenberg and During, 1997).



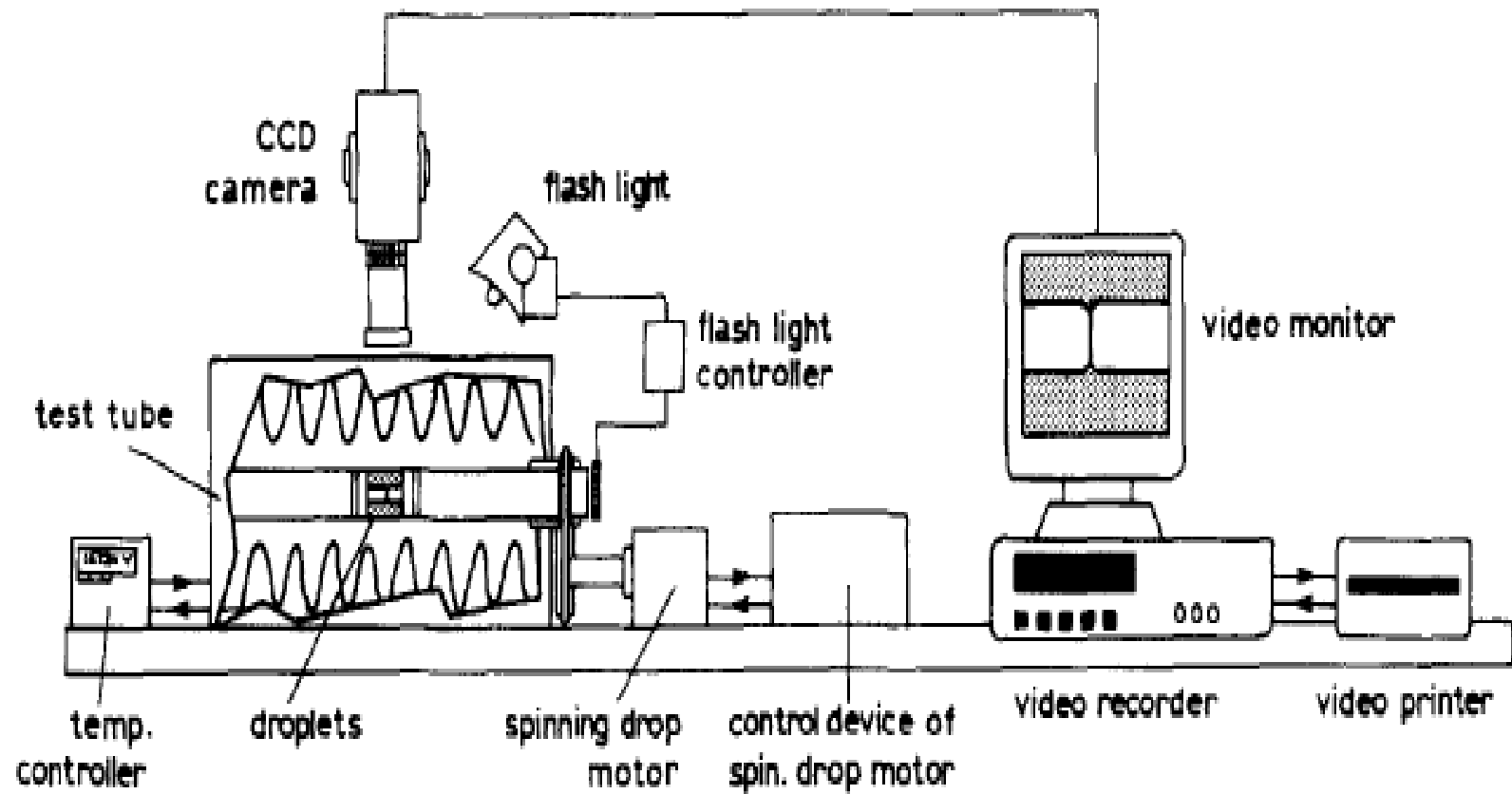
**Figure 11.** (a) Two droplets in the spinning drop chamber. (b) After deformation to the quasi-static situation ( $R_c$  contact radius,  $R_d$  outer radius). (c) After coalescence. (Schoolenberg and During, 1997).

A Vonnegut equation is applied to calculate the IFT from the equilibrium shape.

$$\sigma = \Delta\rho\omega^2 R_e^3/4$$

Where  $\Delta\rho$  is the density difference between the two phases,  $\omega$  is the speed of rotation and  $R_e$  the equilibrium droplet radius.

The SDT experimental chamber consists of a quartz cylinder which is rotated with a speed up to  $2100 \text{ rad.s}^{-1}$ . The chamber can be heated to  $400^\circ\text{C}$ . The quartz cylinder is surrounded by thermal insulation except for a small window, where the droplets can be observed and can be videotaped through a microscope. The length of the cylinder is 150 mm and its internal diameter 5 mm. It contains a calibrating rod to determine the refractive index of the matrix at the measurement temperature. For the two-droplet experiment the chamber is additionally filled with glass rods to reduce its length to *ca.* 10 mm.



**Figure 12.** Spinning Drop Technique Apparatus. (Schoolenberg and During 1997).

## 2. LITERATURE REVIEW

Since the very beginning of humanity, the demand of energy has been increasing day by day. Since oil is an important source of energy, increasing oil production has been essential. As mentioned previously, many ways have been investigated to EOR, chemical injection is one of the methods that has been used recently (Donaldson *et al.*, 1989).

### 2.1. Chemical Injection

More than 50% of oil remains in the well after the first and secondary recovery because of high viscosity of oil. In order to increase the oil production IFT must be lowered, and to obtain that, several chemicals such as CO<sub>2</sub>, alkaline solutions, polymers, alcohol, and surfactant had been used to decrease the IFT.

#### 2.1.1. Carbon dioxide (CO<sub>2</sub>) Injection

CO<sub>2</sub> is used to enhance oil recovery, where it is injected into oil wells. CO<sub>2</sub> main advantage is that usually most of oil wells are in a supercritical conditions, where CO<sub>2</sub> acts as both a pressurizing agent and most likely develops the miscibility with oil, reduces its viscosity, and IFT which enabling the oil to flow more rapidly through the earth to the removal well. In mature oil fields, extensive pipe networks are used to carry the carbon dioxide to the injection points (Sohrabi *et al.*, 2011).

#### 2.1.2. Alkaline solutions

Alkaline solution injection is an EOR process, increasing the pH by adding relatively inexpensive alkaline agents such as sodium hydroxide (NaOH), potassium hydroxide (KOH), sodium ortosilicate (Na<sub>4</sub>SiO<sub>4</sub>), and sodium carbonate (Na<sub>2</sub>CO<sub>3</sub>) of the injected

water. The alkaline reacts with certain crude oil constituents, emulsify oil and water, change rock wettability and solubilize interfacial films, and decrease oil IFT, all these mechanisms eventually will increase oil recovery. Although the process may be simple compared with other chemical injections but it is complex, due to the needs of a detailed lab evaluation and careful selection of a reservoir to apply (Tuřksoy and Baęci, 2000).

### **2.1.3. Polymers in EOR**

Water-soluble polymers are used in many oil field operations; the role of the polymer is to increase the viscosity of the aqueous phase, which can improve the oil recovery. However, technical and economic factors restrict the using of it in practical application and it is not favorable to use with oil viscosity higher than 200 mPa s. due to the need of very high concentration of polymer (Wang and Dong, 2009).

### **2.2. Surfactant in EOR**

Surfactants are amphiphilic compounds which can reduce surface tension and IFT by accumulating at the interface of immiscible fluids and increase the solubility, mobility, and subsequent biodegradation of hydrophobic or insoluble organic compounds. Chemically synthesized surfactants are commonly used in the petroleum, food and pharmaceutical industries as emulsifiers and wetting agents. Surfactants also play an important role in enhanced oil recovery by increasing the apparent solubility of petroleum components and effectively reducing the IFT of oil and water (Singh *et al.*2007).

Scientific methods were introduced for formulating ultra low IFT systems for enhanced oil recovery. The recovery activity was judged by the solubilization of crude oil and the Em droplet size formed by the crude oil and the surfactant solutions. The solubilization capacity was evaluated using UV absorption measurement. Spinning drop apparatus was employed

in determining the ultra low IFT. It was found that a surfactant system which can achieve ultra low IFT had the three characteristics:

First: the surfactant solution contains micelles of around 100 nm in size; secondly, the surfactant solution has high solubilization power; finally, the Em formed by the surfactant solution and crude oil had droplet size below 200 nm (Chiu and Kuo, 1999).

Among the various surfactants, sulfonates or petroleum sulfonates have been widely used in EOR. Historically, these sulfonates came as a byproduct of white oil manufacturing.

Different methods were investigated to reduce the amount of surfactant requirements in ME systems. Several variables can be changed to reach the lowest IFT possible, such as temperature, salinity, and chain length, while the hydrophobic or hydrophilic part of the surfactant can be modified to achieve this goal, such as introducing an extended surfactants, and the addition of co-surfactant to our active system, like alcohol and cationic surfactant (Donaldson *et al.*, 1989).

### **2.2.1. Temperature effect**

Temperature plays an important role in forming ME, sometimes at the same surfactant concentration, increasing temperature shifts the phase behavior to Winsor III phase (Pashley and Karaman, 2004).

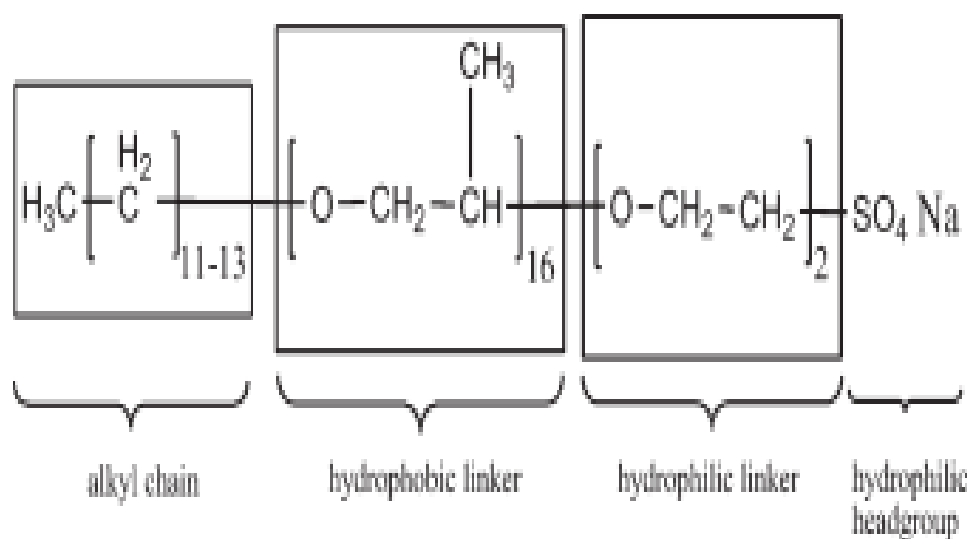
### **2.2.2. Chain effect (Extended Surfactants)**

In 1948 P.A. Winsor showed that ME solubilization capacity of water and oil can be improved by increasing the oil-surfactant and water-surfactant interactions. He also found that it can be possible to have a micellar/reverse micellar solution containing large amounts of oil/water with low viscosity. Optimum solubilization can be found when the interactions are equal between oil and water. Therefore there are two possibilities to increase the



interaction between oil/water effectively, either by increasing the hydrophilicity of the head group of the surfactant, or the hydrophobicity of the tail group. In the 1980, there were ideas to enhance solubilization in ME by using block copolymer additives, or by introducing molecules that bridge the bulk phase and the adsorbed surfactant layer, this can be done by using what is called lipophilic and hydrophilic "linker effect". In both cases the purpose is to modify an extended zone in the water and oil domains close to their boundary.

Using the linker effect, new kinds of surfactants (extended surfactants) was recently used. These types of surfactants contain hydrophilic/lipophilic linkers to stretch further into the oil and water phase, in order to enhance the solubility of oil in water. Studies showed that the lipophilic amphiphilic additive improves and decrease the IFT and therefore increase the solubilization of oil, by extending the hydrophobic part of surfactant with PO deeper into the oil phase near the interface, (e.g. X-AES) (Figure 13). Some extended surfactants were compared with conventional surfactant having similar hydrophilic head and hydrocarbon tail. For example  $C_{12,13}-(PO)_8-SO_4Na$  were investigated against  $C_{12}-SO_4Na$  which is known as Sodium Dodecyl Sulfonate (SDS), and found that the extended surfactant decreased the IFT more efficiently (Klaus *et al.*, 2009)(Sabatini *et al.*, 2010).

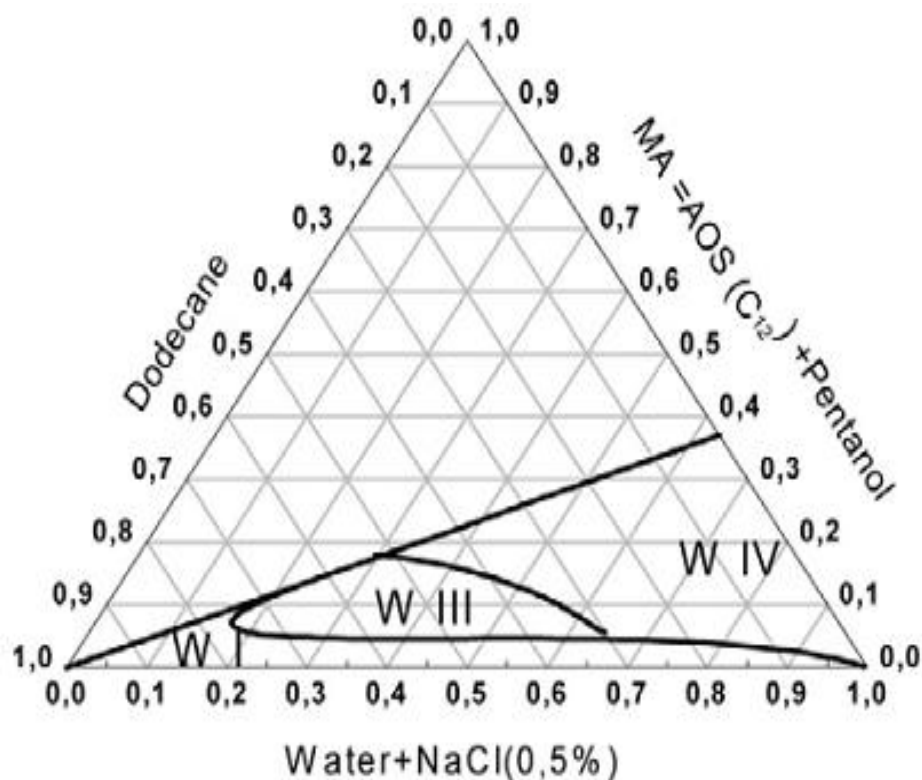


**Figure 13.** Structure of extended surfactant X-AES. (Klaus *et al.*, 2009)

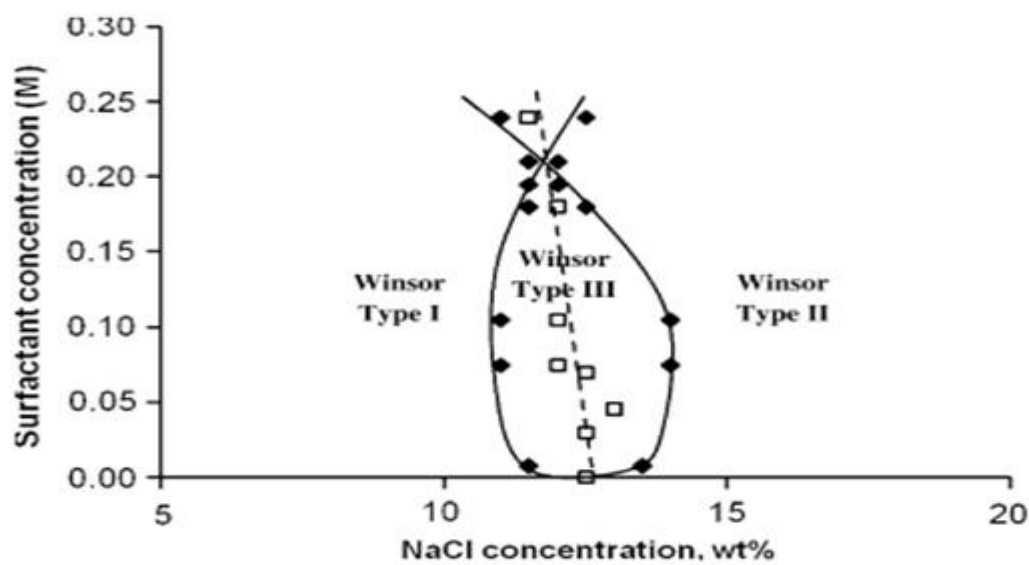
### 2.2.3. Salinity effect

Many researches show that the IFT is strongly dependent on the salinity of the aqueous phase, and IFT approaches its minimum value at a critical salt concentration. A low IFT value appeared when combining low concentration of a particular petroleum sulfonate with high salt concentration and paraffinic crude, other scans were done with naphthenic crude, and found that the Winsor region shifted, it is obvious that to approach the low IFT a specific concentration of surfactant, and salinity must be used (Donaldson *et al.*, 1989).

The salinity effect and the hydrocarbon chain length of surfactant have also been studied using three types of ( $\alpha$  olefinesulfonates of sodium) (AOS) with a general formula of  $[\text{R}-(\text{CH}_2)_n-\text{CH}=\text{CH}_2]$ , where  $n$  is the number of carbons. Phase diagrams of  $\text{C}_{12}$ ,  $\text{C}_{14}$ ,  $\text{C}_{16}$ , were determined with salinity and was found that  $\text{C}_{12}$ , has the best results, with low concentration of the surfactant, and the introduction of  $\text{NaCl}$  into the system which gives a broad field of existence of ME (Figure 12) (Nedjhioui *et al.* 2007)



**Figure 14.** Effect of NaCl (0.5%) on phase behavior. (Nedjhioui *et al.* 2007)



**Figure 15.** Fish diagram of the C<sub>12,13</sub>-(PO)<sub>8</sub>-SO<sub>4</sub>Na, brine water/hexadecane ME at 27°C and equal volume of oil to water (Sabatini *et al.*, 2010)

#### 2.2.4. Co-surfactant effect

A developed ME system based on using an efficient surfactants and interfacially active co-surfactants, efficient anionic surfactants and glycol ether co-surfactants that are stable to temperature and compositional changes and yet employ low levels of non-volatile surfactants. These ME systems are finding utility in a range of applications, in consumer and industrial cleaning formulations, chemical reaction media, polymerization, and active ingredient delivery. In EOR using surfactants alone will not decrease IFT effectively (Klier *et al.*, 2000).

##### 2.2.4.1. Alcohol using

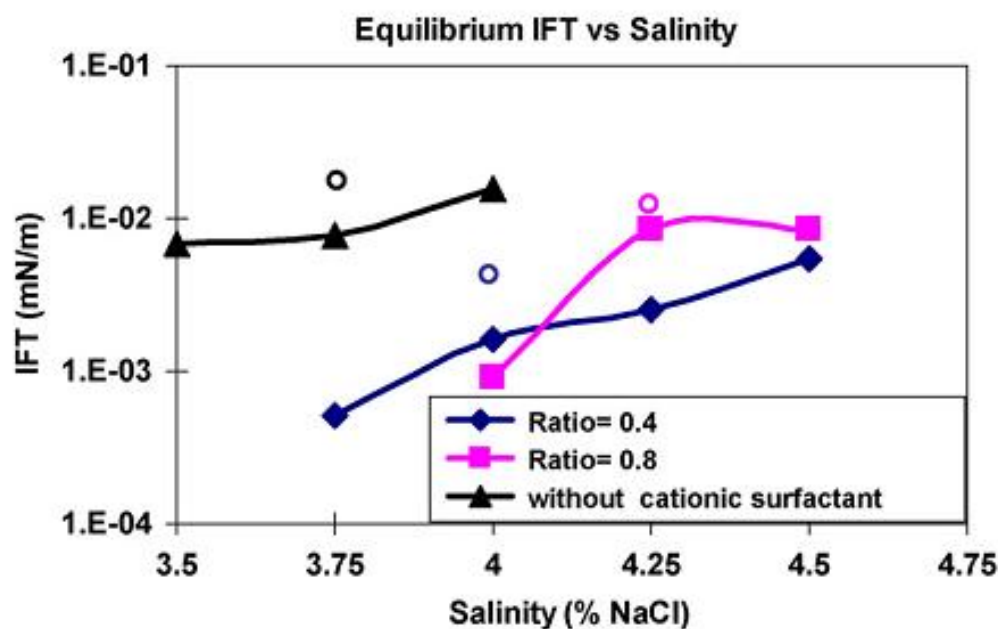
Alcohol used as a co-surfactant, resulting of making a middle phase ME, and in some cases can reduce the IFT up to 0.01 mN/m and sometimes less. Many types of alcohol had been tested such as linear aliphatic alcohols, branched aliphatic alcohols, aliphatic cyclic alcohols, and aromatic alcohols to determine the optimum alcohol chain length and in a research it was found that 1-octanol has the lowest IFT values when tested with alkyl polyglycoside surfactants. However, alcohol affects the stability of the ME. When adding alcohol with same chain length as surfactant it would stabilize the ME, but destabilize when adding alcohol with higher or lower chain length. Besides many do not prefer using alcohol due to its toxicity and high flammability, and some alcohols do not decrease the IFT value so efficiently (Shiao *et al.* 1998) (Stefan *et al.*, 2009).

##### 2.2.4.2. Cationic surfactant

Surfactant films with long, straight hydrocarbon chains of uniform length promote high solubilization of oil and low IFT's if ME form. However, such films tend to be rigid and form the lamellar liquid crystal. Increasing temperature or adding alcohol may disorder the

film and makes it flexible but it is not always preferred and feasible. Nevertheless films can be more disordered and hence more flexible without adding alcohol by: (1) using surfactants with branched hydrocarbon chains such as ethylene or propylene oxide chains or (2) adding another surfactant with different tail structure, for instance a much shorter hydrocarbon chain length such as TBAB.

A phase behavior of free alcohol mixture of anionic and cationic surfactants was determined. The cationic surfactant amounts was mainly smaller than the anionic, with crude oil, adding sodium carbonate ( $\text{Na}_2\text{CO}_3$ ) to convert the naphthenic acid into soap, the salinity scan showed that using small amount of cationic surfactant decreased the IFT values and increased oil solubilization (Kayali *et al.* 2010).



**Figure 16.** Effect of adding cationic surfactant on IFT

### **Aim of the Present Work**

This study is investigating the phase behavior using of extended surfactant, which is sodium polypropylene oxides sulfate,  $C_{12-13}H_{25-27}(PO)_4$ ,  $(L_{123} - 4S)^{\circledR}$  consisting of a branched hydrocarbon chain, water and n-decane, in addition of short chain cationic surfactant TBAB as a co-surfactant for EOR, to be used. Therefore, the objectives of this study can be summarized as following:

- 1) Determination the phase behavior of oil/ water/ surfactant using n-decane as oil model.
- 2) Determination the phase behavior of n-decane/ water/ surfactant, co-surfactant.
- 3) Formulating the middle phase ME by salinity scan for n-decane and crude oil.
- 4) Measuring the IFT values for the middle phase ME.

### 3. MATERIALS AND METHODS

#### 3.1. Materials

The following materials had been used:

- The extended surfactant used in this work was a sodium polypropylene oxides sulfate,  $C_{12-13}H_{25-27}(PO)_4SO_4$ , (L<sub>123</sub> – 4S)<sup>®</sup> consisting of a branched hydrocarbon chain. It is 32.5 wt% active with 0.1 wt % Na<sub>2</sub>SO<sub>4</sub>, 2.5 wt % free oil and 64.9 wt % water. The surfactant was donated by Sasol North America Inc. (West lake, Louisiana).
- TBAB 98%, and n-decane 99% were obtained from Sigma.
- Sodium chloride 99%, and sodium carbonate 99% were from Merck.
- Crude oil sample was provided from Jordan Petroleum Refinery Company.
- Deionized water.

All chemicals were used without further purification.

#### 3.2. Instrumentation

The following instruments were used:

- Precisa 410AM-FR Balance
- Vacuum jar 12" Nitrile and Viton.
- Vibrofix VFI Electronic (Shaker)
- Labofuge 200 Heraeus centrifuge with maximum speed of 5300 revolutions/ min
- Rotating shaker
- Spinning-drop tensiometer (SITE 04, Kruss).

### 3.3. Methods

#### 3.3.1. Preparing the Surfactant

The  $(L_{123} - 4S)^{\circledR}$  sample provided was 32.5% active and in order to determine as much as possible from phase behavior, the increasing of  $(L_{123} - 4S)^{\circledR}$  concentration was essential, a sample of the surfactant was put in vacuum jar at 25 °C overnight. The maximum concentration reached was 65%, because any increase above that percentage will make the surfactant separate into two phases.

#### 3.3.2 Phase Diagram Determination

In order to determine the location and boundaries of the different phases on the ternary phase diagram titration method were used to determine the first partial ternary phase diagrams of anionic extended surfactant  $(L_{123} - 4S)^{\circledR}$  alone in presence of water and n-decane. Samples were prepared by adding n-decane to a pre weighed mixtures at certain percentage of surfactant and water in glass test tubes, which were then sealed by flame, put in centrifuge at 2500 rpm for 5 minutes, then left to equilibrate at 25 °C for one week. Following equilibrium, the samples were checked for phase separation and birefringence. Polarized light was used to detect birefringence, since this distinguishes between anisotropic lamellar and hexagonal liquid crystal and the isotropic (non birefringent) micellar or cubic liquid crystal. Nine samples of  $(L_{123} - 4S)^{\circledR}$  / water combination were prepared in the range of (10-65%) of  $(L_{123} - 4S)^{\circledR}$  in water by air evaporation of water from the  $(L_{123} - 4S)^{\circledR}$  stock solution to get the desired percentage of  $(L_{123} - 4S)^{\circledR}$  in water since we have 32.5% of  $(L_{123} - 4S)^{\circledR}$  standard solution in water. The lower percent of  $(L_{123} - 4S)^{\circledR}$  (lower than 32.5%) was obtained by dilution of  $(L_{123} - 4S)^{\circledR}$  stock solution with



water. Table 2 represents the sample mass and the percentage of  $(L_{123} - 4S)^{\text{®}}$  and water used in phase diagram determination for n-decane.

**Table 2. Mass and percent for  $(L_{123} - 4S)^{\text{®}}$  and water used in phase diagram determination**

Decane			
$(L_{123} - 4S)^{\text{®}}$		Water	
Mass / g	Percent	Mass / g	Percent
0.1014	10.1	0.9006	89.9
0.2056	20.1	0.8192	79.9
0.3014	29.8	0.7088	70.2
0.4022	39.9	0.6064	60.1
0.4566	49.5	0.5272	50.5
0.5046	50.1	0.5008	49.9
0.5552	55.1	0.4512	44.9
0.6012	59.9	0.4012	40.1
0.6536	65.3	0.3478	34.7

In order to save chemicals the second phase was determined by preparing a 65%  $(L_{123} - 4S)^{\text{®}}$ , combined with the cationic hydrotrope, (TBAB), and n-decane in certain ratios, then titrated with water. Table 3 represents the sample mass and the percentage of 65%  $(L_{123} - 4S)^{\text{®}}$  and n-decane used in phase diagram determination.

**Table 3. Mass and percent for 65% (L<sub>123</sub> – 4S)<sup>®</sup> and n-decane used in phase diagram determination**

Water			
65% (L <sub>123</sub> – 4S) <sup>®</sup> , 1:1M(TBAB)		Decane	
Mass / g	Percent	Mass / g	Percent
0.1072	10.6	0.9033	89.4
0.2057	20.4	0.8038	79.6
0.3075	30.3	0.7083	69.7
0.4011	39.9	0.6032	60.1
0.5072	49.9	0.5096	50.1
0.6068	59.8	0.4087	40.2
0.7047	69.9	0.3029	30.1
0.8045	79.9	0.2023	20.1
0.9024	89.9	0.1010	10.1

### 3.3.3. Salinity Scan

Samples of mixtures of various W/W percentage of (L<sub>123</sub> – 4S)<sup>®</sup>, 1:1M ratio of TBAB with various NaCl (0-5)% W/W and water in 10 mL glass test tubes with screw caps was prepared, shaken with a vortex for 1 - 2 minutes. The appearance of the solution was checked visually for transparency and between cross polarizers for birefringence. After that, the model oil (n-decane) was added at specific brine/n-decane weight ratio of one (WOR = 1) and the tubes were gently mixed on a mixer for 12 hours. Then the tubes were placed in an upright position and allowed to settle. The same procedure were done using crude oil instead of n-decane, with adding 1% W/W of sodium carbonate in order to convert the naphthenic acid inside the crude oil to soap, which leads to increase the solubilization of oil in the mixture.

### 3.3.4. IFT measurements

The ultra low interfacial tensions were measured using a spinning-drop tensiometer (SITE 04, Kruss) owned by the Institute of Physical Chemistry, University of Kolon,

Kolon, Germany. Interfacial tensions as low as  $10^{-5}$  mN/m could be measured. For measuring the interfacial tension  $\sigma_{ab}$  between the brine (a) and the oil (b), and  $\sigma_{ac}$  between the middle phase (c) and brine (a). The capillary was filled with brine phase using a 2 ml syringe, avoiding any air bubble to enter the inlet side, at a low speed of rotation of 1000 rpm. The rotation was then interrupted in order to inject 0.2 – 0.3  $\mu$ l from the oil phase or the middle phase using  $\mu$ l syringe through the inlet side. The rotation was then restarted and the injected drop was centered by tilting the capillary and the diameter was measured. The interfacial tension was calculated using Vonnegut equation which considered the injected oil drop to have the form of a cylinder with radius  $r$  and length  $l$ .

$$\sigma = \frac{1}{4}(\rho_1 - \rho_2)\omega^2 r^3 \text{ for } l \gg r \quad (1)$$

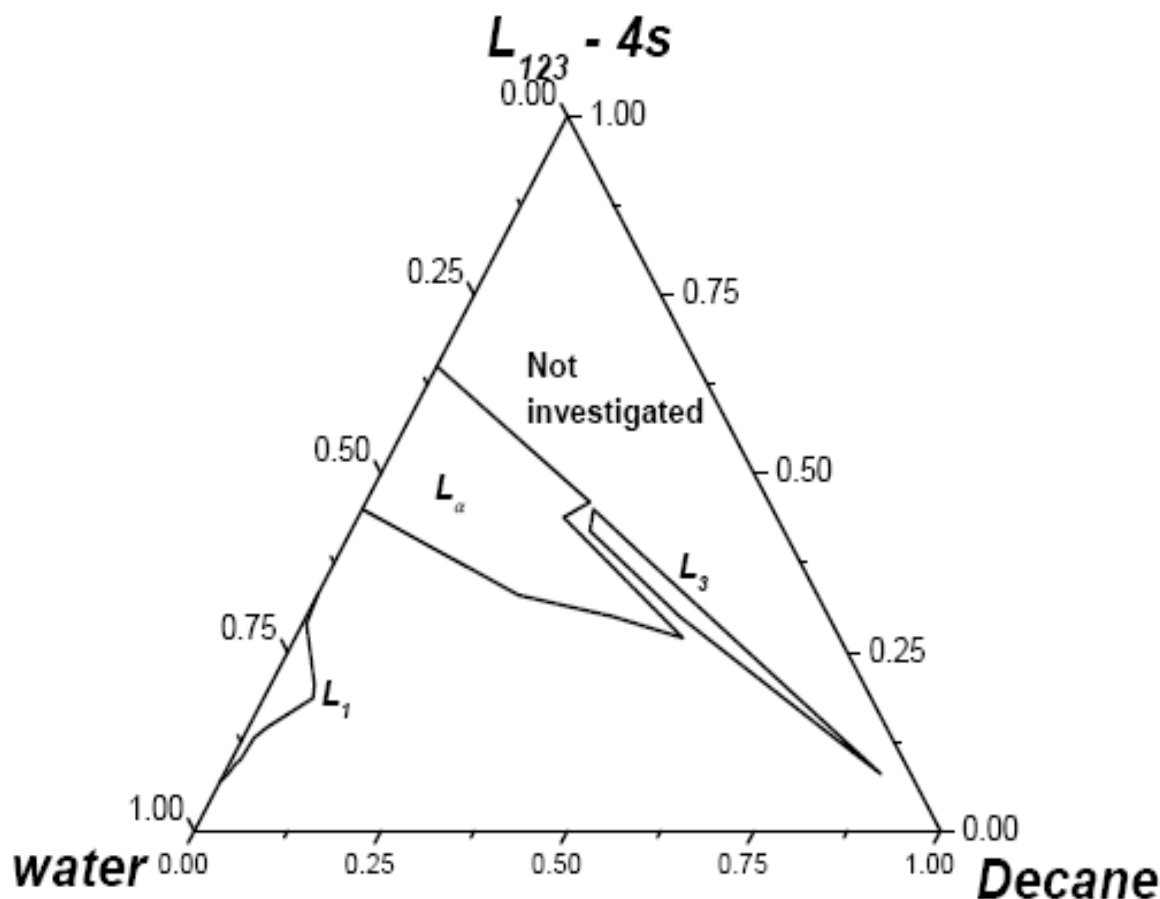
Where  $(\rho_1 - \rho_2)$  is the density difference of the two phases and  $\omega$  the angular velocity.

## 4. Results and Discussion

The results are reported in the following order; first the phase diagrams of (L<sub>123</sub>- 4S)<sup>®</sup>, water, n-decane with and without TBAB, followed by a comparison between the two of them, second the salinity scan of ( L<sub>123</sub>- 4S)<sup>®</sup>, n-decane with (WOR=1), with and without TBAB using various wt% of surfactant and NaCl and a comparison between them. Third the salinity scan (L<sub>123</sub>- 4S)<sup>®</sup>, TBAB (1:1 M ratio) with (WOR=1) using crude oil and various wt% of surfactant and NaCl.

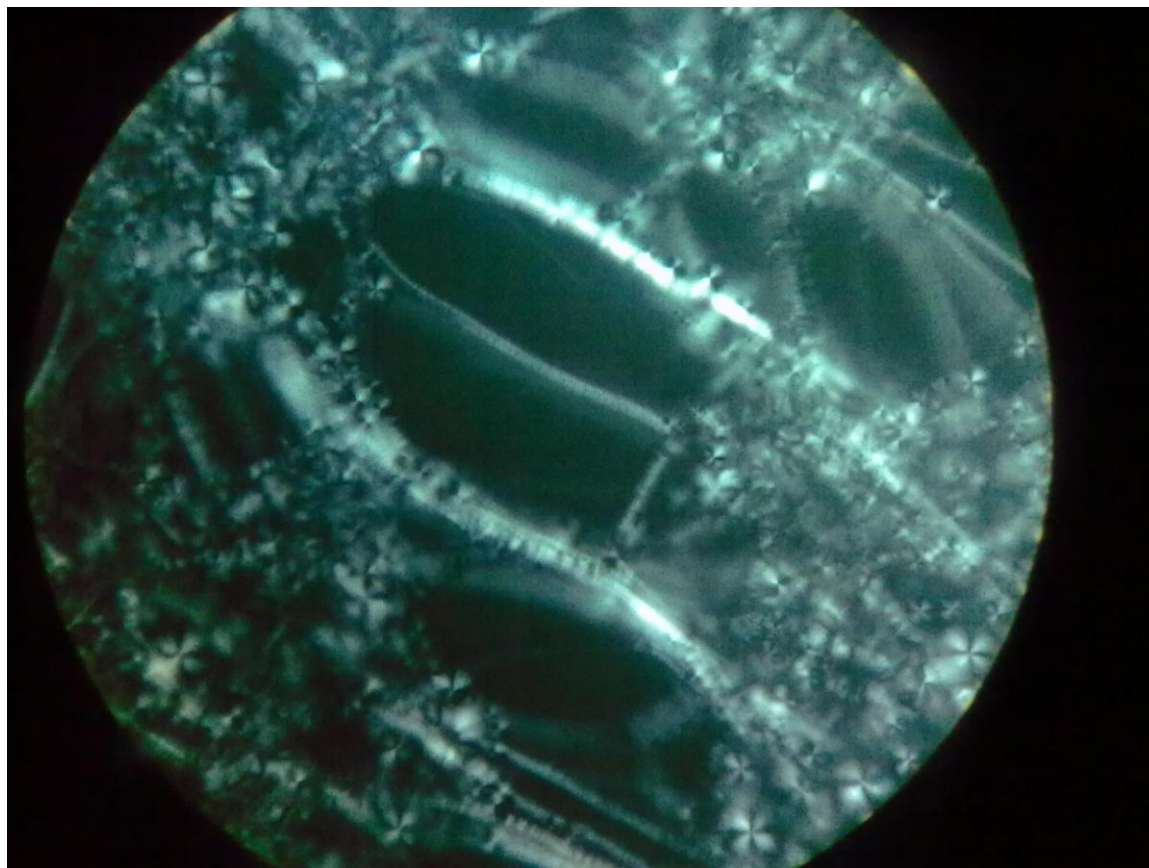
### 4.1. Oil model Decane

The phase behavior of the system (L<sub>123</sub>- 4S)<sup>®</sup>, water, and n-decane was investigated at 25 °C is shown in Figure 17.



**Figure 17.** The partial ternary phase diagram of the system  $(L_{123}-4S)^{\circledR}$ , water and decane.  $L_{\alpha}$ : Lamellar liquid crystal,  $L_3$ : isotopic sponge phase,  $L_1$ : isotopic micellar phase.

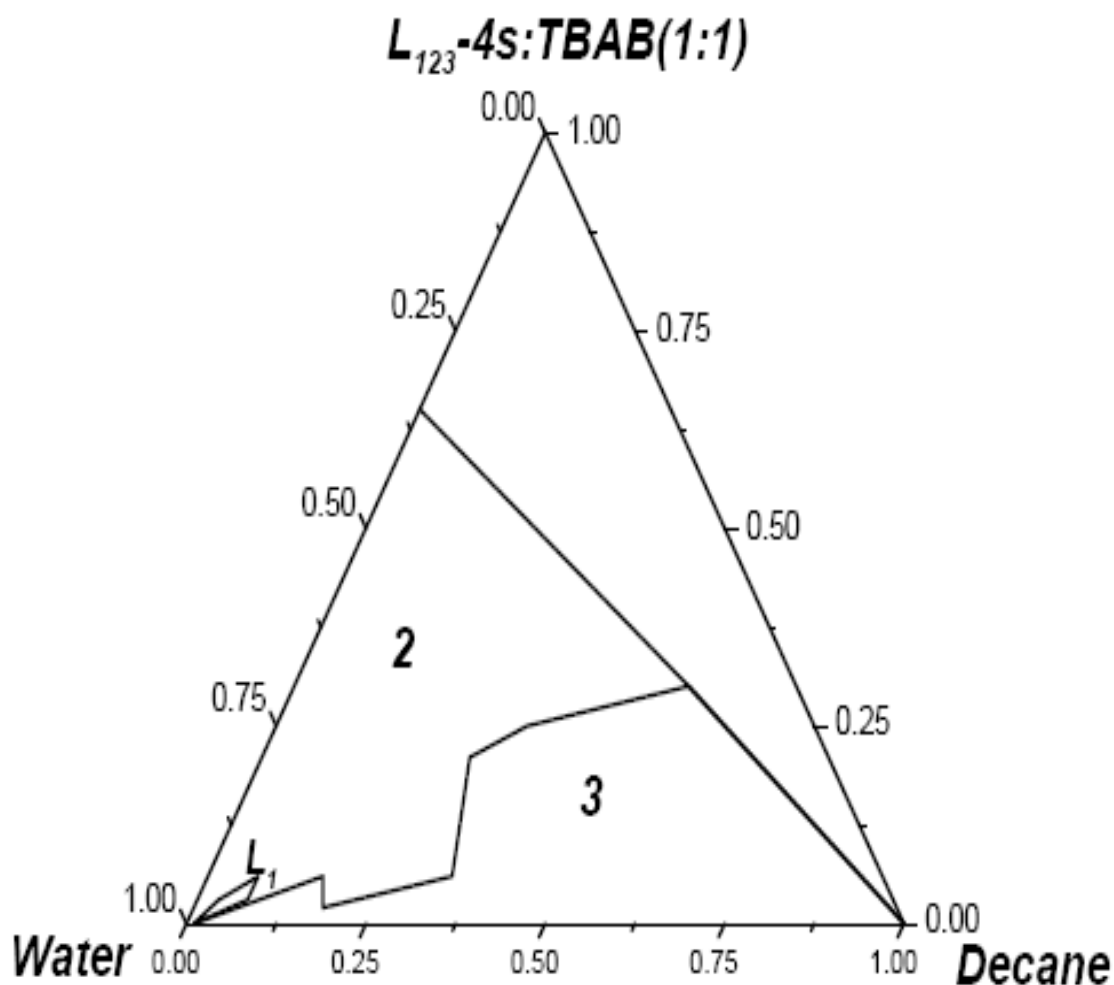
Only partial phase diagram was investigated, because it was not feasible to reach more than 65 wt % of  $(L_{123}-4S)^{\circledR}$ , noticed that it was provided in 32.5% pure, and had to be evaporated to reach the maximum percentage. The phase diagram showed a three of one phase regions. Lamellar liquid crystal  $L_{\alpha}$  covered a wide area at the binary system from 0.55 : 0.45 to 0.35 : 0.65. weight ratio of water :  $(L_{123}-4S)^{\circledR}$  respectively. The area was thinned as n-decane was added to the system, solubilizing up to 62% of n-decane. Figure 18 shows a typical lamellar liquid crystal,  $L_{\alpha}$ , presented in Figure 17 without using the cationic TBAB.



**Figure 18.** Lamellar liquid crystal,  $L_\alpha$

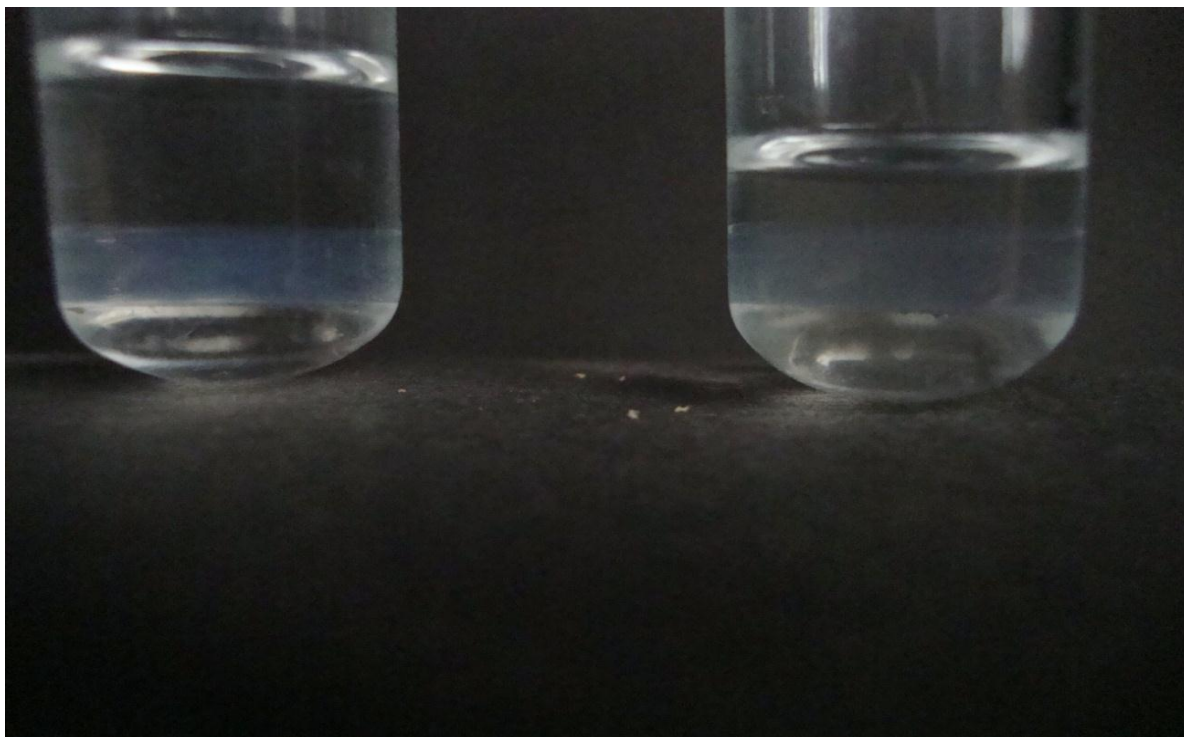
The second region was isotropic sponge phase  $L_3$ , started at 0.3 : 0.4 water :  $(L_{123}-4S)^\circ$  weight ratio solubilizing an amount of 30% up to 95% n-decane. The third phase was the isotropic micellar phase  $L_1$  which appeared at the binary system between 0.93: 0.07 to 0.71: 0.29 water:  $(L_{123}-4S)^\circ$ , solubilizing up to 6.6% to 95% n-decane.

The second phase diagram for the system  $(L_{123}-4S)^\circ$  : TBAB, water and n-decane was determined as shown in Figure 19.



**Figure 19.** The phase diagram of the system  $(L_{123} - 4S)^{\circ} : TBAB$ , water and decane  $L_1$ : isotropic micellar phase, 2: two phase region, 3: three phase region.

In this phase diagram two (2) and three (3) phase regions were appeared, the  $L_{\alpha}$  and  $L_3$  had totally disappeared and the only one region phase appeared was the isotropic liquid solution  $L_1$ . The two phase region shows an emulsion over transparent liquid. The three-phase region here has a bluish middle phase as shown later in Figure 20, indicating a ME formation compared to the three-phase region in first phase diagram in which it shows an emulsion between two transparent liquids (Figure 21).



**Figure 20.** The three phase region in  $(L_{123}-4S)^{\circ}$ , (1:1M TBAB), water and decane system, showing the bluish middle phase.

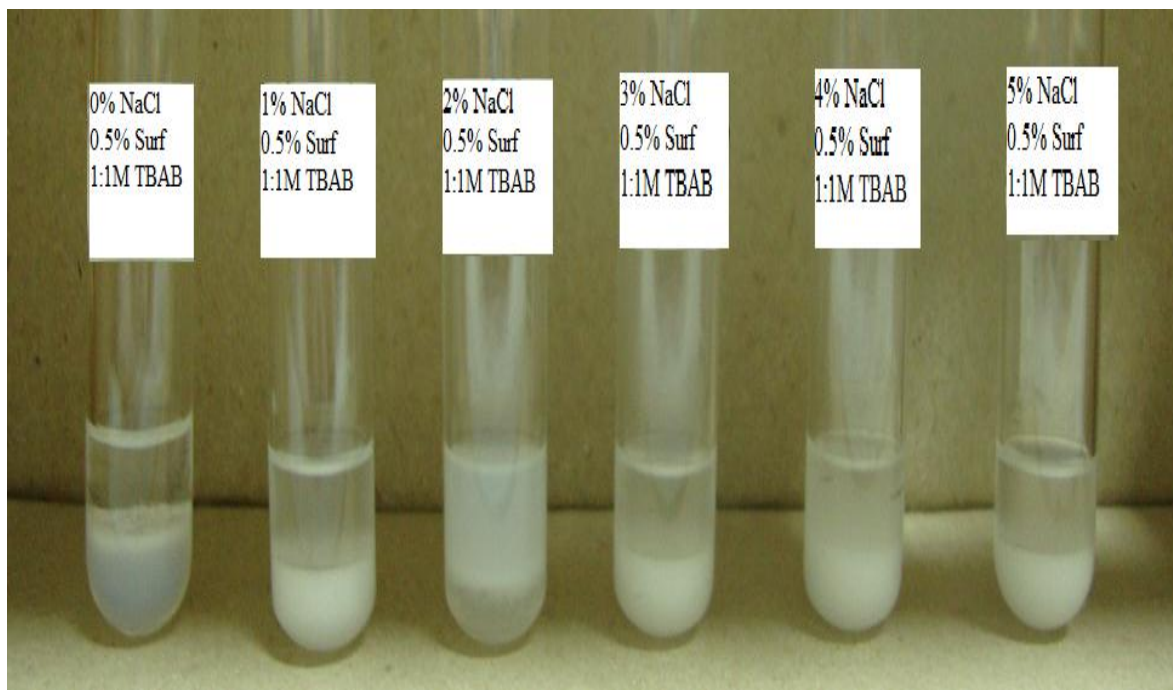


**Figure 21.** The three phase region in  $(L_{123}-4S)^{\circ}$ , water and n-decane system.



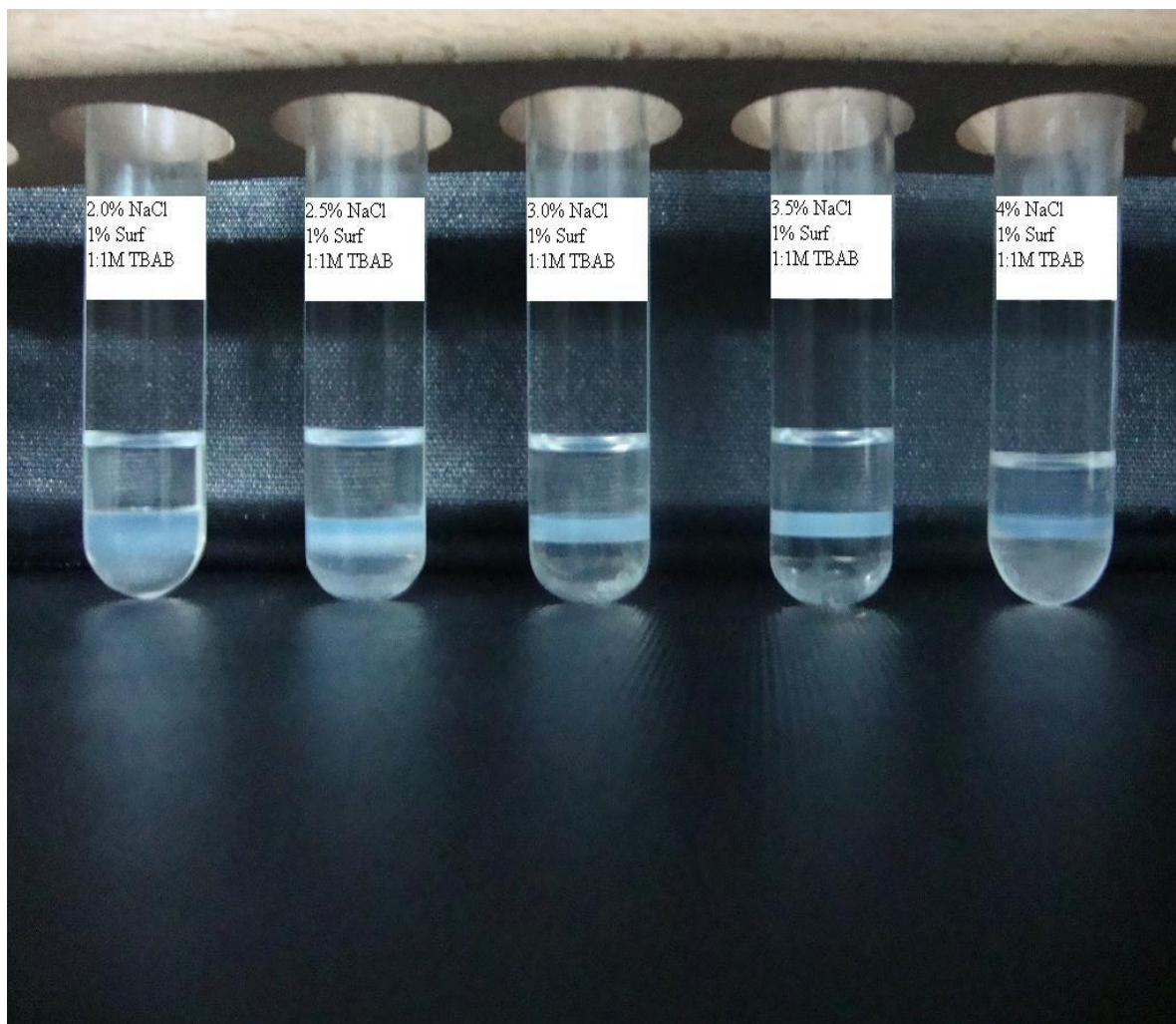
## 4.2. Salinity scan with Decane

Phase behavior at ambient temperature of salinity scan containing 0.5 wt% and 1.0 wt% ( $L_{123-4S}$ )<sup>®</sup>, TBAB (1:1 molar ratio), (0%-5%) NaCl, and scan containing 0.5 wt% ( $L_{123-4S}$ )<sup>®</sup>, (0%-5%) NaCl with equal weight ratios of water and n-decane, were investigated. The salinity scan of 0.5 wt% did not show any Winsor behavior as shown in Figure 22.



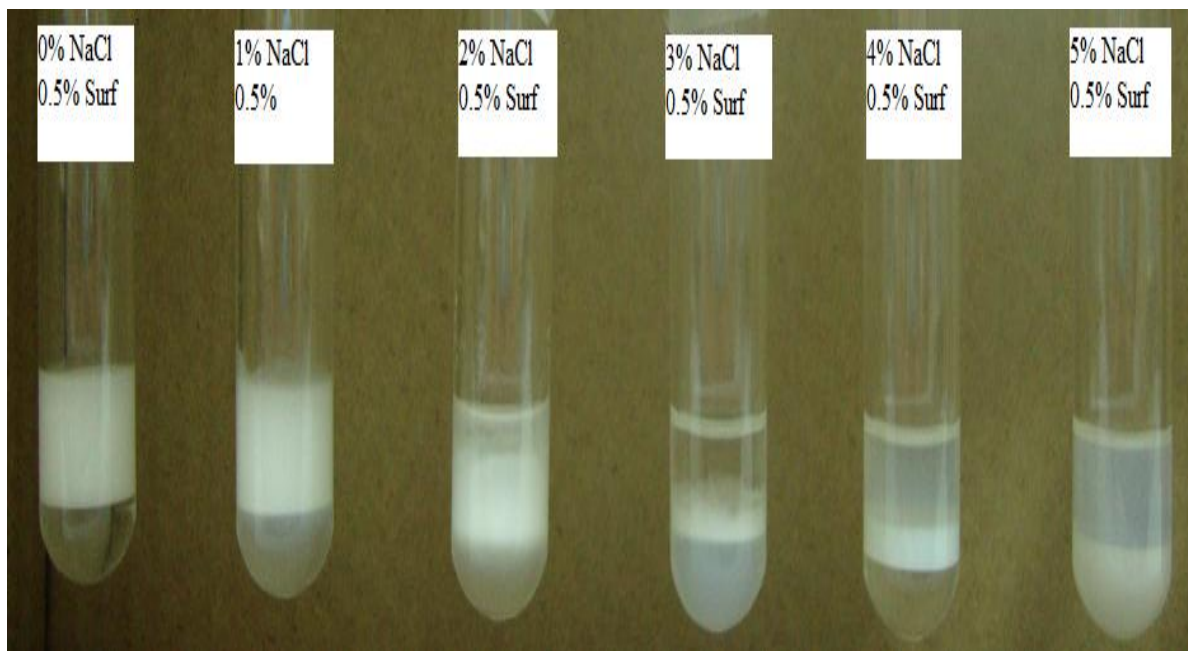
**Figure 22.** Salinity scan containing 0.5 wt % ( $L_{123-4S}$ )<sup>®</sup>, TBAB (1:1 M ratio) with (WOR=1).

The salinity scan of 1.0 wt% ( $L_{123-4S}$ )<sup>®</sup>, TBAB (1:1 molar ratio) showed typical Winsor I, III, II and ME sequence with the middle phase, showing optimum at 2.5 wt% NaCl. Equilibrium time was reached within 6 hours as shown in Figure 23.



**Figure 23.** Salinity scan containing 1.0 wt % ( $L_{123}-4S$ )<sup>®</sup>, TBAB (1:1 molar ratio) with (WOR=1) and n-decane, showing a typical Winsor I, III, II, ME sequence with the middle phase.

The scan of 0.5 wt% ( $L_{123}-4S$ )<sup>®</sup> with the absence of the TBAB showed a middle phase, but was only an emulsion transition with white milky middle phase as shown in Figure 24.



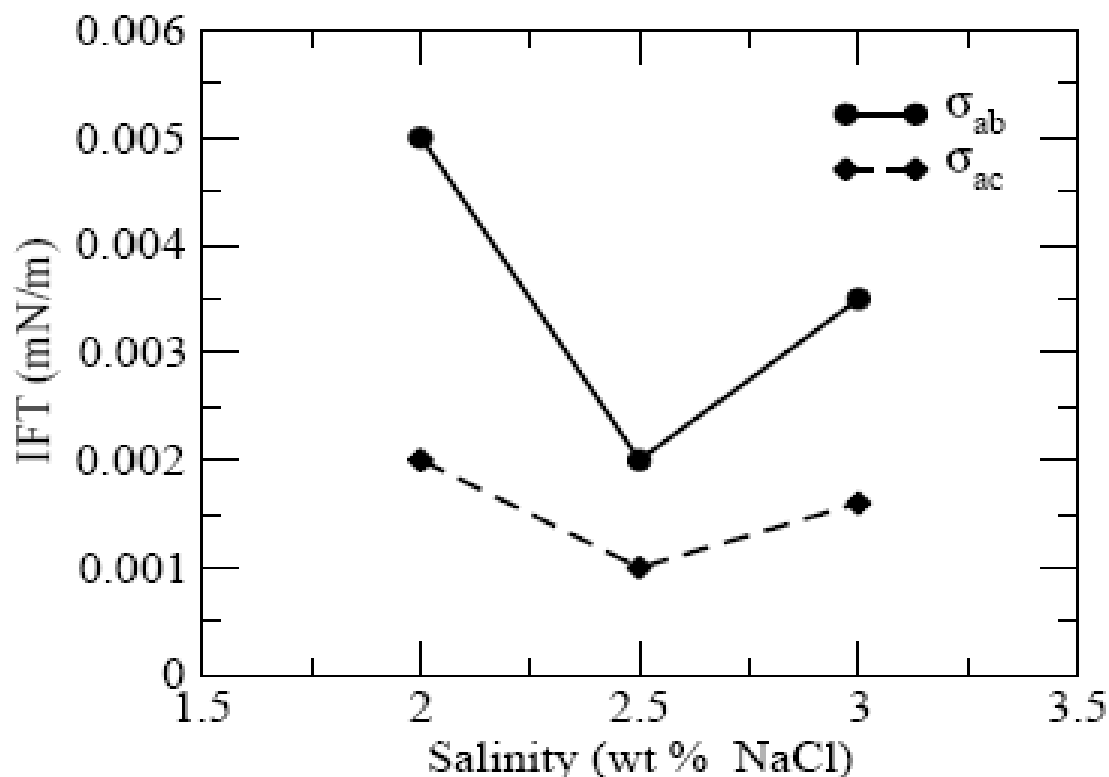
**Figure 24.** Salinity scan containing 0.5 wt %  $(L_{123-4S})^{\circledR}$  with (WOR=1) in absence of TBAB.

**Table 4.** Phase behavior of  $(L_{123} - 4S)^{\circledR}$  with 1:1M TBAB in various NaCl %.

Sample	Surfactant wt%	Co-surfactant (TBAB) ratio	NaCl scan results (phase behavior)
$(L_{123} - 4S)^{\circledR}$	0.5%	0	0%-5% shows emulsion transition with milky phase
$(L_{123} - 4S)^{\circledR}$	0.5%	1:1M	0%-5% didn't show any Winsor behavior
$(L_{123} - 4S)^{\circledR}$	1.0%	1:1M	0%-2% under optimum 2.5% middle phase 3%-5% over optimum

The result of the salinity scan suggested that using very low surfactant percent such as 0.5% would not form the middle phase.

IFT values were measured between the middle phase ME and excess brine,  $\sigma_{ac}$ , and between excess decane and brine,  $\sigma_{ab}$ , using spinning drop technique. At 2.5 wt% NaCl IFT reached a minimum value of 0.001 mN/m for  $\sigma_{ac}$ , and 0.002 mN/m for  $\sigma_{ab}$ , as shown in Figure 25:



**Figure 25.** IFT for the system 1.0wt % ( $L_{123-4S}$ )<sup>®</sup>, TBAB (1:1), decane  $\sigma_{ab}$ : excess decane and brine,  $\sigma_{ac}$ : middle phase ME and brine

In previous research (Kayali *et al.*, 2010) when combining ( $L_{123-4S}$ )<sup>®</sup> with polypropylene oxide quaternary ammonium chloride, known as variquat cc – 9<sup>®</sup> similar ultralow values were obtained. These results demonstrated that we can make use of synergistic effect resulting from the interaction of cationic and anionic head groups in formulating alcohol free ME

Using a branched and short chain cationic hydrotrope like TBAB and variquat cc-9<sup>®</sup>, with (L<sub>123</sub>-4S)<sup>®</sup> will increase the spacing between the long tails of anionic surfactant leading to more oil solubilization, also those short chain hydrotropes promoted rapid equilibrium time, compared when using alcohol.

According to (De Gennes and Taupin, 1982), the characteristic length  $\xi$  can be calculated by:

$$\xi = 6 \frac{\varphi(1-\varphi)}{\varepsilon} \quad (1)$$

Where  $\varphi$  is the volume fraction,  $\varepsilon$  is the total internal interface per unit volume which can be calculated by:

$$\varepsilon = N_c a_c = \frac{\varphi_c}{V_c} a_c \quad (2)$$

Where  $N_c$  is the number density of surfactant in the middle phase,  $a_c$  is the mean area occupied by each molecule,  $\varphi_c$  is the surfactant volume fraction, and  $V_c$  is the volume of surfactant molecule.

Using De Gennes approximation, for equal volume ratio of water and oil,  $\varphi = 0.5$ , and assuming  $\frac{V_c}{a_c} \cong 1nm$ , we will get

$$\xi = \frac{1.5 \times 10^{-9}}{\varphi_c} \quad (3)$$

Applying this equation to our middle phase ME formulated with (L<sub>123</sub>- 4S)<sup>®</sup>, TBAB, assuming all the surfactant is present in the middle phase, which is in this case 3.3 wt % Surf. will give  $\xi = 45.5 nm$

ME with characteristic length  $\xi$  is stable if

$$\sigma_{ab} \xi^2 = 0.44 kT \quad (4)$$

Where  $k$  is Boltzman constant. (Sottmann and Stray, 1998)

Applying this equation to our result with  $\xi = 45.5$

$$\sigma = 8.7 \times 10^{-4} \text{ mN/m}$$

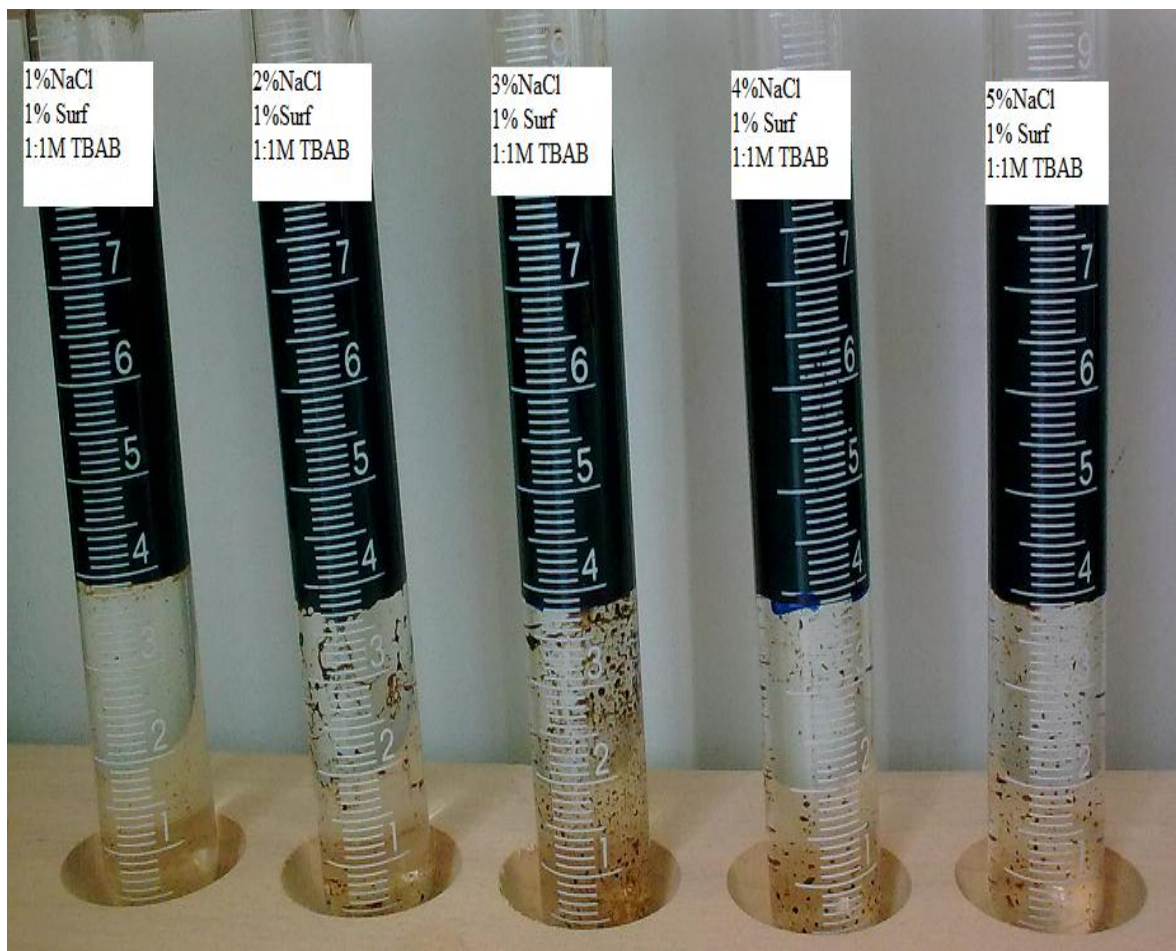
This calculated value is almost half the IFT value obtained experimentally for the same sample at the optimum salinity of 2.5 wt % NaCl. This value of IFT suggested high rigidity due to the steric hindrance caused by the presence of PO groups inside the extended surfactant.

### 4.3. Salinity scans with crude oil

The result of the salinity scan with the model oil n-decane showed that introducing short chain cationic hydrotrope like TBAB increases the solubilization of oil with rapid equilibrium time, which makes this method may be capable to be used in EOR.

The salinity scan containing 0.5 wt % (L<sub>123</sub>-4S)<sup>®</sup> with (WOR=1), using crude oil did not show any middle phase behavior, only two phase appeared one is liquid the other was emulsion, its volume was varied along the NaCl %, also after 11 days the two phase returned to two phase oil and liquid as shown in Figure 26.





**Figure 26.** The salinity scan behavior after 11 days, showing two phase oil and liquid.

The salinity scan containing 1.0 wt% ( $L_{123-4S}$ )<sup>®</sup> 1:1M (TBAB) with WOR=1, using crude oil showed under optimum behavior at 4% NaCl Figure 27, but last for 9 days.



**Figure 27.** Salinity scan containing 1.0 wt % ( $L_{123}-4S$ )<sup>®</sup>, TBAB (1:1 molar ratio) with WOR=1 and crude oil.

The salinity scan of the crude oil shows that this method may be used in EOR and the difference of the behavior from model oil may be explained due to the presence of many oil compounds inside the crude oil.



## 5. Conclusion

The partial ternary phase diagram of the system (L<sub>123</sub>-4S)<sup>®</sup>, water, and n-decane was determined at 25 °C showed a huge area of lamellar liquid crystalline phase  $L_\alpha$  and a sponge phase  $L_3$ , which both disappeared completely when combining TBAB to (L<sub>123</sub>-4S)<sup>®</sup>. The three phase region using only (L<sub>123</sub>-4S)<sup>®</sup> showed an opaque emulsion middle phase that turned into a bluish transparent middle phase when TBAB was added to the surfactant.

Salinity scan revealed that equimolar ratios of TBAB added to 1.0 wt % (L<sub>123</sub>-4S)<sup>®</sup> produced typical Winsor I, III, II sequence.

Using spinning drop tensiometer, IFT, was measured between the middle phase ME and excess brine ( $\sigma_{ac}$ ) and between decane and brine  $\sigma_{ab}$ . Ultra low IFT values were obtained with  $\sigma_{ab} = 2.0 \times 10^{-3}$  N/m. The characteristic length,  $\xi$ , was calculated using De Gennes approximation and was found 45.5 nm. Using this value, the calculated  $\sigma_{ab}$  was equal to  $8.7 \times 10^{-4}$  mN/m, almost half the experimental value.

The salinity scan of the crude oil showed that this method might be used in EOR, but need to consider many factors that may affect the formation of the middle phase, including temperature, surfactant concentration, and time to reach equilibrium.

## **Future Work**

From the salinity scan results, one can study the effect of temperature, concentration influence of (L<sub>123</sub>-4S)<sup>®</sup> and salt, in crude oil sample. Taking into consideration the source of the crude oil, when applying the technique to real samples, paying attention on the time needed for samples to reach equilibrium.

## References

- Anjum, A. Guedeau-Boudeville, M-A. Stubenrauch, C. and Ahmed Mouchid, A. (2008), Phase Behavior and Microstructure of Microemulsions Containing the Hydrophobic Ionic Liquid 1-Butyl-3 methylimidazolium Hexafluorophosphate, **The Journal of Physical Chemistry B**, 113(1), 239-244.
- Bozey, A.A. (2008), **Method Development for Analysis Of Linear And Branched Alkyl Benzene Sulfonates And Comparison Of Their Phase Behavior In Water And Oil Ternary Systems**, Unpublished Master Thesis, University of Jordan, Amman.
- Chiu Y.C., and Kuo P.R. (1999). An empirical correlation between low interfacial tension and micellar size and solubilization for petroleum sulfonates in enhanced oil recovery. **Colloids and Surfaces A: Physicochemical and Engineering Aspects**. 152, 235-244.
- Davis, E.R., Frey, R., Sarquis, M., and Sarquis L.J. (2006), **Modern Chemistry**, (2<sup>nd</sup> ed.), Texas: Holt, Rinehart and Winston.
- De Gennes, P.G. and Taupin, C. (1982), Microemulsions and The Flexibility of Oil/Water Interface, **J. Phys. Chem.**, 86, 2294-2304.
- Donaldson, C.E. Chilingarian, V.G. and Yen, F.T. (1989), **Enhanced Oil Recovery, II, Processes and Operations**, (2<sup>nd</sup> ed.), New York: Elsevier Science Publishing Company INC.
- Erbil, H. Yidirim (2006), Surface **Chemistry of Solid and Liquid Interfaces**, (1<sup>st</sup> ed.), Oxford: Blackwell Publishing Ltd.
- Fernandez, P. Andre, V. Rieger, J. and Kuhnle, A. (2004), Nano-emulsion Formation by Emulsion Phase Inversion, **Colloids and Surfaces A: Physicochemical Engineering Aspects**, 251, 53-58.
- Gluyas, G.J. and Swarbrick, E.R. (2004), **Petroleum Geoscience**, (1<sup>st</sup> ed.), Massachusetts: Blackwell Science Ltd.
- Holmberg, K. Jonsson, B. Kronberg, B. and Lindman, B. (2002), **Surfactant and polymers in aqueous solution**, (2<sup>nd</sup> ed.). England: John Wiley & Sons Ltd.
- Huang, T. (1995), **Microemulsions, Emulsions and Liquid Crystals Implications in Cosmetics and Fragrances**, Unpublished PhD. Thesis, Clarkson University, New York.
- Iglauer, S. Wu, Y. Shuler, P. Tang, Y. and Goddard III, A. W. (2009), Alkyl polyglycoside surfactant-alcohol Cosolvent Formulations for Improved Oil Recovery, **Colloids and Surfaces A: Physicochemical Engineering Aspects**, 339, 48-59.

Inaya, A.M.A.H. (2008), **Microemulsion Preparations (middle phase) for Surfactant Enhancing Aquifer Remediation**, Unpublished Master Thesis, Al-Quds University, Jerusalem.

Kayali, H.I., Liu, S., and Miller, A.C. (2010), Microemulsions Containing Mixtures Of Propoxylated Sulfates With Slightly Branched Hydrocarbon Chains And Cationic Surfactants With Short Hydrophobes Or PO Chains, **Colloids and Surfaces A: Physicochemical Engineering Aspects**, 354, 246-251.

Kayali, I., Qamhieh, K., and Olsson, U. (2011), Formulating Middle Phase Microemulsions Using Extended Anionic Surfactant Combined with Cationic Hydrotope, **Journal of Dispersion Science and Technology**, 32, 41-46.

Kegel, K.W. and Lekkerkerker, N.W.H. (2002), Competition Between a Lamellar and a Microemulsion Phase in an ionic Surfactant System, **The Journal of Physical Chemistry B**, 97(42), 11124-11133.

Klaus, A. Tiddy, J.T.G. Touraud, D. Schramm, A. Stuhler, G. Drechsler, M. and Kunz, W. (2010), Phase Behavior of an Extended Surfactant and a Detailed Characterization of the Dilute and Semidilute Phases, **Langmuir Article**, 26(8), 5435-5443

Klier, J., Tucker, C.J., Kalantar, T.H., and Green D. P. (2000). Properties and Applications of Microemulsions. **Advanced Materials**, 12(23), 1751-1757.

Laidler, J.K. Meiser, H.J. and Sanctuary, C.B. (2003), **Physical Chemistry**, (4<sup>th</sup> ed.), Chicago: Houghton Mifflin Harcourt.

Lopez-Montilla, C.J. Pandey, S. Shah, and O.D. Crisalle, D.O. (2005), Removal of non-ionic Organic Pollutants from Water via liquid-liquid Extraction, **Water Research**, 39, 1907-1913.

Meinardus, W.H., Dwarakanath, V., Ewing, J., Hirasaki, J.G., Jackson, E.R., Jin, M., Ginn, S.J., Londergan, T.J., Miller, A.C., and Pope, A.G. (2002), Performance Assessment of NAPL Remediation in Heterogeneous Alluvium, **Journal of Contaminant Hydrology**, 54, 173-193.

Nedjhioui, M., Canselier, J.P., Mostefa, N.M., Bensmaili, A., and Skender, A. (2007). Determination of micellar system behavior in the presence of salt and water-soluble polymers using the phase diagram technique. **Desalination**, 206, 589-593.

Pashley, R. and araman, M. (2004), **Applied colloid and surface chemistry**, (1<sup>st</sup> ed.). England: John Wiley and Sons Ltd.

Rieger, M. M. and Rhein, L. D. (1997), **Surfactants in cosmetics**, (2<sup>nd</sup> ed.). New York: Marcel Dekker.

Salager, J. (1999), **Surfactants-Types and Uses**, (Version # 2). Merida-Venezuela: Laboratorio FIRP.

Salager, J-L. (2002), **Surfactants: Types and Uses**, (2<sup>nd</sup> ed.), Merida: Universidad De Los Andes.

Schoolenberg, E.G. and During, F. (1998), Coalescence and Interfacial Tension Measurement for Polymer Melts: A Technique Using the Spinning Drop Apparatus, **Polymer**, 39(4), 757-763.

Sen, R. (2010), **Biosurfactants**, (1<sup>st</sup> ed.), Texas: Landes Bioscience and Springer Science+Business Media, LLC.

Shiao, S.Y., Chhabra, V., Patist, A., Free, M.L., Huibers, D.T., Gregory, A., Patel, S., Shah, D.O. (1998). Chain length compatibility effects in mixed surfactant systems for technological applications. **Advances in Colloid and Interface Science.**, 74, 1-29.

Shiaw, Y.S. Chhabra, V. Patist, A. Free, L.M. Huibers, D.T.P. Gregory, A. Pate, S. and Shah, O.D. (1998), Chain Length Compatibility Effects in Mixed Surfactant Systems for Technological Applications, **Advances in Colloid and Interface Science**, 74, 1-29.

Singh A., Van Hamme, J.D., and Ward O.P. (2007). Surfactants in microbiology and biotechnology: Part 2. Application aspects. **Biotechnology Advances**, 25, 99-121.

Sohrabi, M. Riazi, M. Jamiolahmady, M. IdahKechut, N. Ireland, S. and Robertson, G. (2011), Carbonated Water Injection (CWI) – A Productive Way of Using CO<sub>2</sub> for Oil Recovery and CO<sub>2</sub> Storage, **Energy Procedia**, 4, 2192-2199.

Sottman, T. and Strey, R. (1997), Ultralow Interfacial Tensions in Water-n-Alkane-Surfactant Systems, **J. Chem. Phys.**, 106, 8606-8615.

Taugbol, K. Van Ly, T. and Austad, T. (1995), Chemical Flooding of Oil Reservoirs 3. Dissociative Surfactant-Polymer Interaction with a Positive Effect on Oil Recovery, **Colloids and Surfaces A: Physicochemical Engineering Aspects**, 103, 83-90.

Taylor C.K. and Nasr-El-Din, A.H. (1998), Water-Soluble Hydrophoically Associating Polymers for Improved Oil Recovery: A literature review, **Journal of Petroleum Science and Engineering**, 19, 265-280.

Tu`rksoy, U. and Bag`ci, S. (2000), Improved Oil Recovery Using Alkaline Solutions in Limestone Medium, **Journal of Petroleum Science and Engineering**, 26, 105-119.

Vazquez-Duhalt, R. and Quintero-Ramirez, R. (2004), **Petroleum Biotechnology, Developments and Perspectives**, (1<sup>st</sup> ed.), New York: Elsevire Science Publishing Company INC.

Wang, J. and Dong, M. (2009), Optimum Effective Viscosity of Polymer Solution for Improving Heavy Oil Recovery, **Journal of Petroleum Science and Engineering**, 67, 155-158.

Witthayapanyanon, A. ThanhPhan, T. Heitmann, C.T. Harwell, H.J. and Sabatini, A.D. (2010), Interfacial Properties of Extended-Surfactant-Based Microemulsions and Related Macroemulsions, **Journal of Surfactant Detergent**, 13, 127-134.

## استخدام مستحلبات ميكرونية تحتوي على سلسلة قصيرة أيونية موجبة و سالبة ذات نشاط سطحي للاستخلاص المعزز للنفط

إعداد  
فؤاد شامل رشدي حبقوقه

المشرف  
الأستاذ الدكتورة عبيد فايز البواب

المشرف المشارك  
الأستاذ الدكتور ابراهيم محمود كيالي

### ملخص

تم تحديد مخطط السلوك الطور الجزئي لنظام ثلاثي مكون من مادة نشطة سطحيا ممددة أيونية سالبة لكبريتات الكل متعدد اكسيد البروبيلين  $C_{12}(PO)_4SO_4$  لوحده مع الماء و ديكان. كما تم تحديد السلوك الطوري لهذه المواد بوجود مادة مساعدة للمادة ذات النشاط السطحي رباعي بيوتيل بروميدات الامونيا (TBAB) ضمن ظروف محيطية.

تم تكوين الطور الوسطي للمستحلب الميكروني (Microemulsion) باستخدام مسح الملوحة (Salinity scan) لمناطق مخففة نسبيا من المادة النشطة سطحيا\محلول ملحي\ديكان ايضا بوجود (TBAB). باستخدام الكشف البصري, و المجهر الضوئي لكشف التباين وتحديد الاطوار المختلفة. تم استخدام جهاز القطرة المغزلية لقياس التوتر السطحي. اظهر مخطط السلوك الطوري الأول باستخدام المادة النشطة سطحيا لوحدها وجود منطقتين من طور واحد, أحدهما مكونة من صفائح بلورية سائلة (Lamellar liquid crystal,  $L_\alpha$ ), و الثانية من طور اسفنجي ( $L_3$  sponge phase). بالإضافة لوجود منطقة مكونة من ثلاثة اطوار من مستحلب (Emulsion) واقع بين سائلين شفافين. اما في مخطط السلوك الطوري الثاني باستخدام المادة النشطة سطحيا مع (TBAB) ظهرت منطقة مذيلة جديدة ( $L_1$  isotropic micellar) مع اختفاء طور  $L_\alpha$  و  $L_3$  تماما , ومنطقة الطور الثلاثي اصبح لديها طور وسطي شفاف مزرق.

اسفرت قياسات التوتر السطحي ما بين الطور الوسطي\المحلول الملحي و ما بين الديكان\المحلول الملحي عن وجود قيم منخفضة جدا. هذه القياسات اقترحت وجود قساوة عالية بسبب عائق الفراغية لوجود مجموعة اكسيد البروبيلين داخل المادة النشطة الممددة سطحيا. قيم التوتر السطحي المحسوبة باستخدام تقريب دي جينز (De Gennes) كانت حوالي نصف القيم المقاسة . اظهرت نتائج الفحص الملحي عن امكانية استخدام هذه الطريقة مع النفط خام.